

# Geochemical Variations during Kīlauea's Pu'u 'Ō'ō Eruption Reveal a Fine-scale Mixture of Mantle Heterogeneities within the Hawaiian Plume

JARED P. MARSKE<sup>1</sup>\*, MICHAEL O. GARCIA<sup>1</sup>,  
AARON J. PIETRUSZKA<sup>2</sup>, J. MICHAEL RHODES<sup>3</sup>  
AND MARC D. NORMAN<sup>4</sup>

<sup>1</sup>DEPARTMENT OF GEOLOGY AND GEOPHYSICS, UNIVERSITY OF HAWAII, HONOLULU, HI 96822, USA

<sup>2</sup>DEPARTMENT OF GEOLOGICAL SCIENCES, SAN DIEGO STATE UNIVERSITY, SAN DIEGO, CA 92182, USA

<sup>3</sup>DEPARTMENT OF GEOSCIENCES, UNIVERSITY OF MASSACHUSETTS, AMHERST, MA 01003, USA

<sup>4</sup>RESEARCH SCHOOL OF EARTH SCIENCES, AUSTRALIAN NATIONAL UNIVERSITY, CANBERRA A.C.T. 0200, AUSTRALIA

RECEIVED AUGUST 15, 2007; ACCEPTED APRIL 21, 2008  
ADVANCE ACCESS PUBLICATION MAY 27, 2008

*Long-term geochemical monitoring of lavas from the continuing 25-year-old Pu'u 'Ō'ō eruption allows us to probe the crustal and mantle magmatic processes beneath Kīlauea volcano in unparalleled detail. Here we present new Pb, Sr, and Nd isotope ratios, major and trace element abundances, olivine compositions, and petrographic data for Pu'u 'Ō'ō lavas erupted from 1998 to 2005. Olivine fractionation and accumulation are important crustal processes for the eruption, with minor clinopyroxene fractionation observed in the most recent lavas. Small, yet systematic variations in  $^{87}\text{Sr}/^{86}\text{Sr}$  and incompatible trace element ratios, and MgO-normalized major element abundances document rapid changes in the parental magma composition delivered to Pu'u 'Ō'ō. Recent (1998–2003) lavas display a systematic temporal evolution towards an intermediate area between the compositional fields of historical Kīlauea and Mauna Loa lavas. At least three distinct mantle source components are required to explain the overall isotopic and chemical variability of Pu'u 'Ō'ō lavas. Two of these source components observed in pre-1998 Pu'u 'Ō'ō lavas have similar Pb, Sr, and Nd isotope ratios, although one underwent a recent (<8 ka) small-degree melting event and became depleted in incompatible trace elements. This recently depleted component was an increasingly important source for lavas erupted between 1985 and 1998. The third component is a hybrid mixture of nearly equal portions of Kīlauea- and Mauna*

*Loa-like mantle source compositions. It was progressively tapped in greater amounts from 1998 to 2003 and then subsequently decreased. The increasing importance of the hybrid source can be explained if melt pathways migrated from an area within Kīlauea's typical melting region (important for the 1985–1998 lavas) towards Mauna Loa, where a similar proportion of Kīlauea- and Mauna Loa-like mantle components might exist. The Pu'u 'Ō'ō data suggest that Kea and Loa mantle components are distributed on a fine-scale within the Hawaiian plume, and both are present beneath Kīlauea volcano. Based on the geochemical and isotopic variations during the Pu'u 'Ō'ō eruption, the estimated volume for Kīlauea and Mauna Loa compositional heterogeneities is <10–35 km<sup>3</sup>.*

KEY WORDS: Hawaii; Kīlauea; volcanoes; geochemistry; mantle heterogeneity

## INTRODUCTION

Time-series studies of geochemical variations during long-lived eruptions or eruptive sequences provide valuable insight into the magmatic processes within active volcanoes (e.g. Arenal, Costa Rica, Bolge *et al.*, 2006;

\*Corresponding author. Telephone: +1-808-956-5960.  
E-mail: marske@hawaii.edu

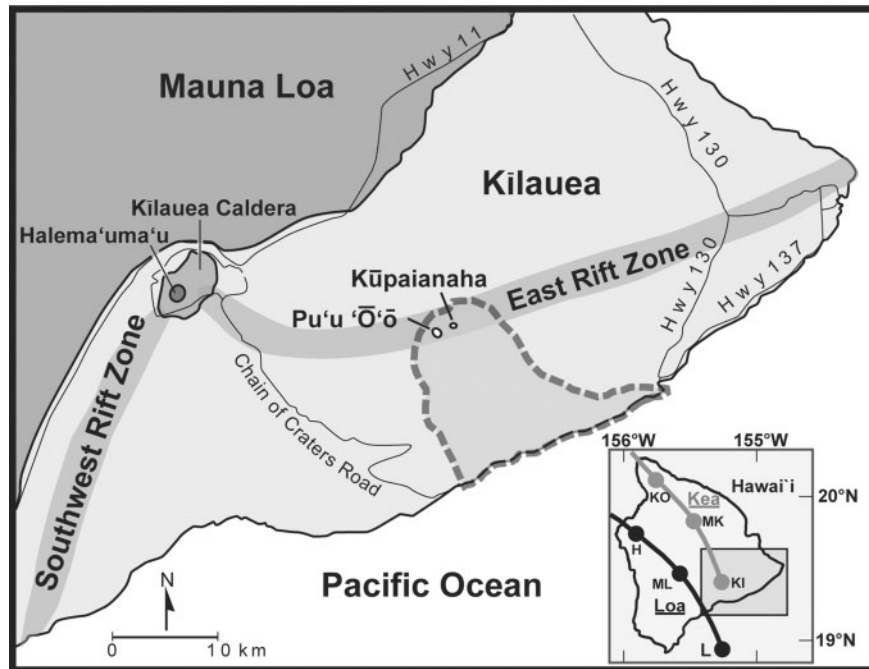


**Fig. 1.** Location map of the Pu'u 'O'o eruption flow field (dashed outline) on the East Rift Zone of Kīlauea volcano, Hawai'i (after Mittelstaedt & Garcia, 2007). Lava erupted from two primary vents: the Pu'u 'O'o cone between 1983 and 1986 and between 1992 and 2007 (episodes 4–47, 50–53, and 55), and at Kūpaianaha between 1986 and 1992 (episodes 48 and 49). The inset map shows the distribution of Loa (H, Hualālai; ML, Mauna Loa; L, Lō'ihi) and Kea (KO, Kohala; MK, Mauna Kea; KI, Kīlauea) volcanoes.

Etna, Italy, Rizzo *et al.*, 2006; Grímsvötn, Iceland, Sigmarsdóttir *et al.*, 1992; Parícutin, Mexico, Wilcox, 1954; McBirney *et al.*, 1987; Piton de la Fournaise, Réunion, Vlastelic *et al.*, 2005). These studies provide a detailed view of the crustal- and mantle-related magmatic processes occurring on short time scales (days to years). Kīlauea volcano, located on the island of Hawai'i (Fig. 1), has erupted ( $\sim 4.3 \text{ km}^3$ ; Macdonald *et al.*, 1983; Sutton *et al.*, 2003) frequently during the past 200 years, making it an ideal location to investigate temporal variations in lava chemistry that are related to changes in mantle source compositions and melting conditions within the Hawaiian plume.

Previous seismic and petrological studies suggest that Kīlauea magmas originate from partial melting at mantle depths  $>60\text{--}80 \text{ km}$  within the upper Hawaiian plume (e.g. Eaton & Murata, 1960; Watson & McKenzie, 1991; Tilling & Dvorak, 1993). Rapid melt extraction from the mantle source region into chemically isolated channels (e.g. McKenzie, 1985; Williams & Gill, 1989) is probably the dominant melt transport mechanism beneath Kīlauea because it provides a relatively large amount of melt for sustained, high-volume eruptions such as Pu'u 'O'o (Pietruszka *et al.*, 2006). After accumulating, these melts are thought to ascend through a primary conduit delivering magma to Kīlauea's shallow (2–6 km deep) magma reservoir, and may subsequently erupt in the summit caldera or feed the volcano's two rift zones (e.g. Tilling & Dvorak, 1993; Wright & Klein, 2006).

The Pu'u 'O'o eruption is the longest sustained (25+ years) and most voluminous ( $\sim 3 \text{ km}^3$  erupted lava) historical eruption of Kīlauea volcano (Garcia *et al.*, 2000; Heliker & Mattox, 2003). Pu'u 'O'o magmas are thought to partially bypass the summit reservoir (based on the rapid variations in incompatible trace element ratios for Pu'u 'O'o lavas compared with Kīlauea summit lavas) before intruding Kīlauea's East Rift Zone to feed a shallow ( $<3 \text{ km}$  depth) magma reservoir system beneath the Pu'u 'O'o cone (Garcia *et al.*, 1996; Shamberger & Garcia, 2006). Since the start of the eruption in January 1983, there have been small but systematic variations in the Pb, Sr, and O isotope ratios and major and trace element abundances of Pu'u 'O'o lavas. These fluctuations provide an unprecedented opportunity to document the crustal processes (e.g. crystal fractionation and accumulation, and crustal assimilation) and mantle source and melting variations (e.g. mantle source heterogeneity, and melt production, extraction, and transportation) within the Hawaiian plume on a time scale of months to years (e.g. Garcia *et al.*, 1989, 1992, 1996, 1998, 2000; Putirka, 1997; Thornber, 2001, 2003; Pietruszka *et al.*, 2006).

Two different length scales of mantle heterogeneity within the Hawaiian plume have been recognized based on the distinct isotopic variations of single volcanoes. Large-scale heterogeneity has been proposed based on the persistent intershield geochemical differences of Hawaiian volcanoes over tens to hundreds of thousands of years

(e.g. Frey & Rhodes, 1993; Chen *et al.*, 1996), and the long-term differences in Pb isotope ratios (Tatsumoto, 1978; Abouchami *et al.*, 2005) along two NW–SE-trending loci of volcanoes (Fig. 1): the northeastern ‘Kea’ trend (e.g. Kilauea) and the southwestern ‘Loa’ trend (e.g. Mauna Loa). The Kea end member is defined by higher  $^{206}\text{Pb}/^{204}\text{Pb}$  and  $^{143}\text{Nd}/^{144}\text{Nd}$  and lower  $^{87}\text{Sr}/^{86}\text{Sr}$  and is predominantly observed in lavas from Kilauea, Mauna Kea, West Maui, and East Molokai volcanoes (Stolper *et al.*, 1996; DePaolo *et al.*, 2001; Blichert-Toft *et al.*, 2003; Eisele *et al.*, 2003; Xu *et al.*, 2007). The Loa end member is defined by higher  $^{87}\text{Sr}/^{86}\text{Sr}$  and lower  $^{143}\text{Nd}/^{144}\text{Nd}$  and  $^{206}\text{Pb}/^{204}\text{Pb}$  and is mostly observed in lavas from Mauna Loa, Hualalai, Lanai, Kahoolawe, West Molokai and Ko‘olau volcanoes (Hauri, 1996; Lassiter & Hauri, 1998; Abouchami *et al.*, 2005; Fekiacova *et al.*, 2007).

Single volcanoes (e.g. Kilauea and Mauna Loa) also record isotopic variations over shorter time scales (years to centuries) that are attributed to partial melting of small-scale compositional heterogeneities within the plume (e.g. Frey & Rhodes, 1993; Kurz *et al.*, 1995; Rhodes & Hart, 1995; Pietruszka & Garcia, 1999a; Marske *et al.*, 2007). Estimates for the size and shape of small-scale heterogeneities range from vertical streaks that are several tens to hundreds of kilometers long (e.g. Farnetani *et al.*, 2002; Eisele *et al.*, 2003; Abouchami *et al.*, 2005) to heterogeneous blobs set in a compositionally distinct matrix (e.g. Frey & Rhodes, 1993; Rhodes & Hart, 1995; Blichert-Toft *et al.*, 2003). A range of vertical length scales for these compositional heterogeneities from 6.5–160 km (Blichert-Toft *et al.*, 2003) to 0.06–12 km (Kurz *et al.*, 2004) have been estimated based on isotopic fluctuations recorded in 550–180 ka Mauna Kea lavas. In contrast, the presence of a pancake-shaped heterogeneity (>18 km wide and <5–10 km thick) has been inferred based on systematic Pb, Sr, and Nd isotopic fluctuations in young prehistoric (<2.6 ka) Kilauea and Mauna Loa lavas (Marske *et al.*, 2007). Unlike these previous studies, which document the size of mantle heterogeneities on a scale of hundreds to thousands of years, the Pu‘u ‘O‘o eruption offers an opportunity to probe the finer-scale compositional variations related to distinctive mantle sources on very short time scales (months to years). Here we provide a comprehensive petrological evaluation of the most recent (1998–2005) Pu‘u ‘O‘o lavas using petrography, olivine and whole-rock chemistry, and Pb, Sr, and Nd isotope ratios, and discuss the compositional evolution of these lavas and their implications for the nature and scale of mantle source heterogeneity within the Hawaiian plume.

## OVERVIEW OF THE PU‘U ‘O‘O ERUPTION

The onset of the eruption (episode 1) in January 1983, began with intermittent fire fountaining along an

8-km-long fissure system in the middle of Kilauea’s East Rift Zone (Wolfe *et al.*, 1987; Garcia *et al.*, 1989; Fig. 1). During episodes 2 and 3, activity was localized to a 1 km section of the fissure system. A central vent, Pu‘u ‘O‘o, was the focus of effusion for episodes 4–47 (June 1983–June 1986). These episodes were generally short-lived (5–100 h) with variable (10–400 m) lava fountaining heights (Garcia *et al.*, 1992; Heliker & Mattox, 2003). In July 1986, the primary vent migrated 3 km downrift from the Pu‘u ‘O‘o cone to the Kūpaianaha lava shield (Fig. 1). This shift coincided with a change in eruptive style from episodic, fire-fountaining events to nearly continuous and gentle effusion (Garcia *et al.*, 1996). Kūpaianaha was the site of nearly continuous lava effusion (episodes 48 and 49) until February 1992, when activity shifted back to Pu‘u ‘O‘o. From February 1992 to January 1997 (episodes 50–53), a shield 60 m high and 1.3 km in diameter was built at Pu‘u ‘O‘o (Heliker *et al.*, 1998). On January 29, 1997, the lava lake inside the Pu‘u ‘O‘o shield suddenly drained, and a 22 h eruption (episode 54) occurred 2–4 km uprift (Harris *et al.*, 1997; Thornber *et al.*, 2003).

Following a 24 day hiatus, episode 55 began, marking the longest (1997–2007) and most voluminous ( $\sim 1.6 \text{ km}^3$ ) effusive interval for this eruption. Episode 55 activity displayed nearly continuous eruption of lava (except for infrequent 1–4 day pauses) from vents on the south and west flanks of the Pu‘u ‘O‘o cone (Garcia *et al.*, 2000; Heliker & Mattox, 2003). The most significant event during episode 55 occurred on September 12, 1999, when magma-induced earthquake swarms and surficial deflation of the Pu‘u ‘O‘o cone were followed by intrusion of magma into the upper East Rift Zone of Kilauea (Nakata *et al.*, 2000). An 11 day hiatus followed as magma supplying the Pu‘u ‘O‘o cone was temporarily diverted to the upper rift zone. Episode 55 ended after a 1 day eruption (episode 56) that occurred  $\sim 6$  km uprift of the Pu‘u ‘O‘o cone in mid-June 2007 (Poland *et al.*, 2008). Following a 2 week pause, lava effusion resumed in early July 2007, and, as of May 2008, lava continues to erupt from a vent 2 km downrift of the Pu‘u ‘O‘o cone.

## PETROGRAPHY

A majority of samples studied here were collected in a molten state and most were quenched in water. The sample label (e.g. 17-Aug-01) is the date it was collected, and in nearly all cases is within a day of when it was erupted. The vast majority of the 1998–2005 Pu‘u ‘O‘o lavas petrographically studied are glassy, strongly vesicular, friable and aphyric to moderately olivine-phyric (<3 vol. % phenocrysts; Table 1). Olivine is almost always the only phenocryst in these samples and is usually small ( $\sim 0.5\text{--}1\text{ mm}$  in diameter), euhedral and undeformed with spinel and glass inclusions. Olivine is somewhat less common ( $\sim 1\text{ vol. \%}$ ) in the 1998–2005 lavas compared

*Table 1.* Modal mineralogy of representative 1998–2005 Pu‘u ‘Ō‘ō lavas

Sample	Whole-rock	Olivine		Clinopyroxene		Plagioclase	Matrix
		MgO (wt %)	ph	mph	ph	mph	mph
21-Jan-98	7.96	0.6	3.6	0.0	0.0	0.0	95.8
13-Feb-99	7.41	0.6	3.4	0.0	1.4	0.2	94.4
19-Jun-99	8.17	0.9	2.5	0.0	0.1	0.0	96.5
11-Aug-99	6.85	0.0	2.0	0.0	0.4	0.6	97.0
27-Oct-99	7.98	0.6	3.8	0.0	0.2	0.4	95.0
4-Jan-00	9.54	3.0	3.2	0.0	1.2	0.8	91.8
21-Jun-00	7.23	2.5	0.6	0.0	1.7	0.6	94.6
4-Aug-00	8.29	2.8	2.6	0.0	1.4	1.0	92.2
8-Apr-01	7.93	1.9	3.7	<0.1	2.8	0.2	91.4
29-Sep-01	6.69	0.0	1.9	0.0	2.0	1.1	95.0
12-Apr-02	8.03	2.8	3.0	0.0	3.0	0.4	90.8
20-Aug-02	8.11	1.6	2.8	0.6	3.0	0.2	91.6
21-Nov-02	7.39	0.6	1.0	0.0	<0.1	0.0	98.4
12-Mar-03	7.53	2.4	2.8	0.0	1.0	0.2	93.6
29-Aug-03	6.87	0.6	1.6	<0.1	0.8	0.2	96.8
15-Jan-04	7.18	1.6	0.6	<0.1	3.0	0.6	94.2
23-Jul-04	6.97	0.6	0.6	0.0	3.0	1.4	94.4
31-Oct-04	6.90	1.8	3.0	0.0	1.4	0.8	93.0
6-Feb-05	7.03	0.8	2.0	0.0	0.8	0.8	95.6
23-Jun-05	6.85	1.0	1.6	0.0	0.4	0.2	96.8

All values are in vol. % and are based on 500 point counts per sample, without vesicles. Phenocrysts (ph) are >0.5 mm long; microphenocrysts (mph) are 0.1–0.5 mm long. Matrix contains glass and crystals <0.1 mm long.

with those from the preceding 6 years of eruptive activity but similar in abundance to lavas erupted from the Kūpaianaha vent (1986–1992; Garcia *et al.*, 1996). The total olivine abundance (phenocrysts and microphenocrysts) generally correlates with whole-rock MgO content, although it can vary ~4 vol. % for a given MgO (Table 1). Clinopyroxene phenocrysts are rare in the 1998–2005 Pu‘u ‘Ō‘ō lavas, yet microphenocrysts of clinopyroxene (up to 3 vol. %) are present in almost all of these lavas (Table 1). In contrast, clinopyroxene is absent or rare (<1 vol. %) in earlier Pu‘u ‘Ō‘ō lavas (except in the more evolved 1983 lavas; Garcia *et al.*, 1992, 1996). Clinopyroxene crystals are small (0.1–0.3 mm), occur commonly in clusters of 3–12 grains, and commonly display sector zoning. Plagioclase microphenocrysts occur in most of the 1998–2005 Pu‘u ‘Ō‘ō lavas, although they are usually rare (<1 vol. %; Table 1) and small (0.1–0.2 mm wide laths). Plagioclase is less common in earlier erupted Pu‘u ‘Ō‘ō lavas (except for the lavas from episodes 1–10 and 54, which were affected by magma mixing in Kīlauea’s East Rift Zone

(Garcia *et al.*, 1989, 1992, 2000; Thornber *et al.*, 2003). The groundmass of the 1998–2005 lavas generally consists of honey-brown glass or black cryptocrystalline material with microlites (<0.1 mm) of plagioclase, clinopyroxene, olivine, and spinel.

## OLIVINE COMPOSITION

A five spectrometer Cameca SX-50 electron microprobe with SAMx automation was used for the olivine analyses at the University of Hawai‘i using techniques described by Garcia *et al.* (2000). Olivine compositions (Table 2) were determined for 175 olivine crystals from 19 lavas erupted between 1998 and 2005 that span a wide compositional range (whole-rock MgO contents of 6.7–9.5 wt %). All of the analyzed olivine crystals are unzoned or normally zoned with up to 3% forsterite (Fo) variation from core to rim. The forsterite content of the olivine cores range from 76.5 to 86.0% (Fig. 2) with phenocrysts and microphenocrysts overlapping in composition. The average Fo content is ~81.1%, which is similar to lavas from the previous 6 years and somewhat lower than olivines in the earlier lavas (1986–1992) erupted from the Kūpaianaha vent (~82.5% on average; Garcia *et al.*, 1996, 2000). The NiO and CaO contents in the olivines are moderate (Table 2) indicating crystallization at crustal depths from somewhat fractionated parental magmas (e.g. Garcia, 2002).

Olivines in the 1998–2005 lavas typically have Fo compositions that are in equilibrium with their whole-rock Mg-number, particularly for lavas with lower Mg-number (<58; Fig. 2). Most samples with Mg-number >58 have olivine compositions that plot below the equilibrium field, especially the sample with the highest Mg-number (4-Jan-00; Fig. 2). The higher Mg-number lavas probably accumulated olivine, which is consistent with their higher abundance of this mineral (e.g. 4-Jan-00 contains the highest olivine content; Table 1). The highest measured forsterite content of olivine within the 1998–2005 lavas (Fo<sub>86</sub>) occurs in a sample with an intermediate Mg-number, 21-Jan-98 (Table 2). This olivine, like all of the other crystals, shows no signs of deformation. Thus, it is probably indicative of the parental magma composition for recent Pu‘u ‘Ō‘ō lavas (Mg-number ~59; Fig. 2), consistent with estimates for previous Pu‘u ‘Ō‘ō lavas (Garcia *et al.*, 2000).

## WHOLE-ROCK ANALYTICAL METHODS

Eighty-two new Pu‘u ‘Ō‘ō lava samples erupted between 1998 and 2005 were analyzed for major and trace element (Rb, Sr, Y, Nb, Zr, Zn, Ni, Cr, V, Ba, and Ce) abundances over a 7 year period using X-ray fluorescence spectrometry (XRF) at the University of Massachusetts (Table 3). The Kīlauea basaltic standards collected from the same flow, K1919 (*n*=13) and BHVO-1 (*n*=13), were run as

*Table 2:* Representative microprobe analyses of olivine cores from 1998–2005 Pu‘u ‘Ō‘ō lavas

Sample	SiO <sub>2</sub>	FeO	NiO	MgO	CaO	Total	Fo	Mg-no.
21-Jan-98	38.89	17.14	0.22	42.46	0.26	98.98	81.5	58.9
	39.16	16.73	0.21	43.01	0.25	99.37	82.1	
	39.74	13.28	0.35	45.64	0.20	99.22	86.0	
13-Feb-99	39.36	18.03	0.18	41.86	0.27	99.64	80.5	57.3
	39.11	16.76	0.22	43.26	0.24	99.59	82.1	
	39.64	15.94	0.26	43.88	0.25	99.96	83.1	
19-Jun-99	39.28	17.22	0.19	42.85	0.25	99.48	81.6	59.4
	39.53	16.96	0.22	42.97	0.26	99.95	81.9	
11-Aug-99	39.13	17.51	0.19	42.40	0.26	99.49	81.2	55.6
	39.27	17.13	0.22	42.79	0.26	99.67	81.7	
	39.31	16.19	0.21	43.45	0.22	99.38	82.7	
4-Jan-00	38.78	17.82	0.16	42.29	0.28	99.34	80.9	62.6
	38.86	17.50	0.21	42.57	0.28	99.42	81.3	
	39.04	17.29	0.19	42.92	0.27	99.72	81.6	
21-Jun-00	38.92	17.82	0.16	42.33	—	99.51	80.9	56.9
	38.95	17.59	0.17	42.55	—	99.51	81.2	
	39.29	17.24	0.18	43.08	—	100.04	81.7	
4-Aug-00	38.72	17.42	0.18	42.47	0.30	99.10	81.3	59.8
	38.69	17.37	0.16	42.59	0.27	99.07	81.4	
8-Apr-01	38.55	19.41	0.16	41.26	0.25	99.64	79.1	58.8
	38.68	18.34	0.16	42.08	0.26	99.53	80.4	
	38.76	17.12	0.20	43.24	0.25	99.57	81.8	
29-Sep-01	38.43	21.55	0.12	39.44	—	99.83	76.5	54.7
	38.88	18.68	0.14	41.62	—	99.61	79.9	
	39.05	17.81	0.18	42.55	—	99.87	81.0	
12-Apr-02	38.87	18.02	0.18	42.26	0.25	99.57	80.7	59.0
	39.10	17.28	0.18	42.75	0.23	99.54	81.5	
	39.45	15.57	0.23	44.04	0.22	99.51	83.4	
20-Aug-02	39.25	17.95	0.23	42.42	0.27	100.13	80.8	59.1
	39.11	17.68	0.20	42.68	0.26	99.94	81.1	
	39.42	16.35	0.20	43.57	0.25	99.79	82.6	
21-Nov-02	39.11	17.99	0.19	42.54	0.25	100.09	80.8	57.1
	39.05	17.43	0.20	42.67	0.27	99.62	81.4	
	39.14	16.86	0.21	43.32	0.25	99.78	82.1	
12-Mar-03	39.26	17.60	0.21	42.35	0.26	99.69	81.1	57.5
	39.08	17.38	0.17	42.27	0.26	99.15	81.3	
	39.02	17.14	0.21	42.46	0.26	99.09	81.5	
29-Aug-03	40.06	17.95	0.16	40.89	0.34	99.41	80.2	55.3
	39.77	17.46	0.19	41.62	0.27	99.30	80.9	
	39.92	17.33	0.14	41.83	0.25	99.46	81.1	

(continued)

*Table 2:* Continued

Sample	SiO <sub>2</sub>	FeO	NiO	MgO	CaO	Total	Fo	Mg-no.
15-Jan-04	39.38	18.25	0.19	41.99	0.27	100.08	80.4	56.5
	39.35	17.60	0.22	42.36	0.26	99.79	81.1	
	39.70	18.44	0.18	41.44	0.26	100.02	80.0	55.9
23-Jul-04	39.79	17.80	0.22	41.96	0.26	100.04	80.8	
	39.43	17.45	0.20	41.89	0.25	99.22	81.1	
	38.35	18.83	0.19	41.52	0.29	99.17	79.7	55.6
31-Oct-04	38.67	18.68	0.23	41.73	0.30	99.61	79.9	
	38.53	18.02	0.25	42.13	0.26	99.19	80.6	
	38.18	19.26	0.19	41.51	0.33	99.48	79.3	56.1
6-Feb-05	38.94	18.64	0.17	41.59	0.27	99.62	79.9	
	39.16	17.07	0.28	42.95	0.27	99.73	81.8	
	38.50	19.03	0.23	41.12	0.30	99.19	79.4	55.4
23-Jun-05	38.85	18.08	0.23	42.00	0.28	99.45	80.5	
	38.92	16.94	0.28	42.95	0.27	99.36	81.9	

Values are the average of three spot analyses per sample. All oxides concentrations are in wt %.

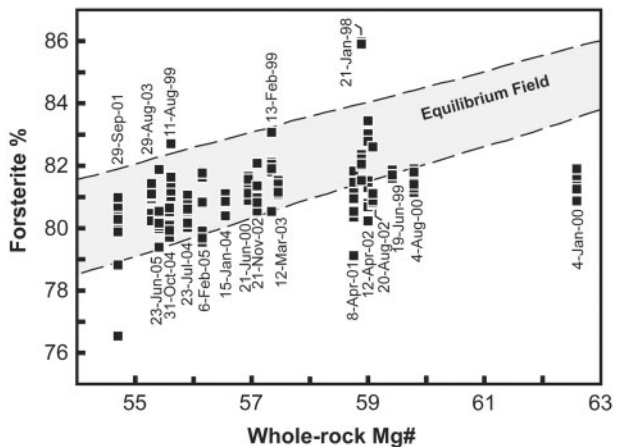


**Fig. 2.** Representative whole-rock Mg-number [ $(\text{Mg}/\text{Mg} + \text{Fe}^{2+}) \times 100$ ] plotted against olivine core forsterite content (Fo %) for 1998–2005 lavas. The Mg-number is calculated assuming 90% of the total iron is  $\text{Fe}^{2+}$ , which is consistent with measurements on Kīlauea lavas (e.g. Moore & Ault, 1965; Byers *et al.*, 1985; Rhodes & Vollinger, 2005). The date with each set of olivine data is the sample number. The diagonal field is the shallow pressure (1 atm) equilibrium field for basaltic magma ( $\text{Fe}/\text{Mg } K_d = 0.30 \pm 0.03$ ; Roeder & Emslie, 1970; Ulmer, 1989). Lava samples that plot below the equilibrium field (e.g. 4-Jan-00) have probably experienced olivine accumulation.

internal controls for major and trace element abundances during this period, respectively (Table 3). All Pu‘u ‘Ō‘ō samples presented here were analyzed in the same XRF laboratory using the same calibration procedures. Thus, any long-term analytical drift in the major and trace element abundances is expected to be relatively minor.

Table 3: Whole-rock XRF analyses of 1998–2005 Pu`u `O`o lavas

Sample	Day	SiO <sub>2</sub>	TiO <sub>2</sub>	Al <sub>2</sub> O <sub>3</sub>	Fe <sub>2</sub> O <sub>3</sub> <sup>*</sup>	MnO	MgO	CaO	Na <sub>2</sub> O	K <sub>2</sub> O	P <sub>2</sub> O <sub>5</sub>	Total	Y	Sr	Rb	Nb	Zr	Ni	Cr	V	Zn	Ba	Ce
17-Jan-98	5493	50.16	2.282	12.70	12.48	0.18	9.26	10.42	2.21	0.402	0.215	100.31	23.2	297	7.0	11.7	139	146	519	273	115	96	28
11-May-98	5607	50.21	2.316	12.80	12.40	0.17	9.10	10.40	2.10	0.405	0.221	100.13	23.5	301	7.1	12.2	142	168	549	274	115	99	26
25-Jun-98	5652	50.54	2.393	13.36	11.98	0.17	7.52	10.95	2.22	0.416	0.232	99.77	24.4	316	6.8	12.4	142	95	465	289	112	100	30
7-Sep-98	5726	50.26	2.353	12.98	12.32	0.17	8.65	10.58	2.24	0.406	0.224	100.16	23.7	306	7.5	12.4	145	145	493	278	115	97	30
14-Nov-98	5794	50.30	2.345	12.99	12.21	0.18	8.38	10.65	2.20	0.409	0.229	99.87	24.0	308	6.4	12.1	140	133	489	283	113	101	27
13-Feb-99	5885	50.58	2.400	13.37	12.14	0.17	7.41	10.91	2.34	0.416	0.235	99.98	24.4	315	7.2	12.5	146	89	385	281	113	97	32
13-Mar-99	5913	50.17	2.344	13.07	12.29	0.17	8.08	10.67	2.30	0.406	0.229	99.70	23.9	306	7.3	12.3	143	120	449	276	114	96	29
13-Apr-99	5944	50.11	2.281	12.79	12.45	0.17	9.03	10.42	2.27	0.393	0.224	100.13	23.2	299	7.1	11.9	140	141	499	270	114	94	28
25-Apr-99	5956	50.47	2.325	13.10	12.17	0.18	8.16	10.65	2.11	0.404	0.225	99.77	24.1	307	6.6	12.0	139	111	450	286	114	99	29
19-Jun-99	6011	50.30	2.324	13.07	12.29	0.17	8.17	10.64	2.28	0.402	0.228	99.87	23.7	305	7.3	12.1	143	119	440	275	114	99	28
14-Jul-99	6036	50.36	2.340	13.10	12.28	0.17	8.03	10.70	2.31	0.402	0.229	99.92	23.9	308	7.4	12.2	143	109	425	277	114	96	30
11-Aug-99	6064	50.66	2.398	13.38	12.04	0.17	6.85	10.98	2.33	0.415	0.232	99.45	24.8	316	7.0	12.6	148	73	327	281	113	90	29
27-Oct-99	6141	50.33	2.320	13.02	12.26	0.17	7.98	10.64	2.36	0.400	0.227	99.71	23.8	307	6.7	12.1	143	105	406	277	114	88	31
20-Nov-99	6165	50.34	2.333	13.13	12.22	0.18	7.69	10.73	2.37	0.402	0.224	99.61	24.0	308	6.9	12.3	144	87	371	273	113	86	29
29-Dec-99	6204	50.39	2.325	13.04	12.28	0.17	7.87	10.65	2.30	0.404	0.227	99.66	24.1	306	6.7	12.0	143	96	404	276	113	83	29
4-Jan-00	6210	49.72	2.217	12.46	12.56	0.18	9.54	10.14	2.24	0.378	0.217	99.64	23.1	292	6.4	11.5	136	140	489	261	113	97	24
19-Feb-00	6256	50.27	2.275	12.87	12.36	0.18	8.55	10.50	2.17	0.386	0.222	99.79	23.7	299	6.7	11.6	138	111	440	270	114	98	27
26-Mar-00	6292	50.83	2.336	13.14	12.21	0.18	7.97	10.75	2.21	0.398	0.225	100.24	23.8	303	6.4	12.0	140	102	419	272	113	100	29
8-Apr-00	6305	50.71	2.388	13.37	11.98	0.18	7.10	11.01	2.36	0.408	0.230	99.73	24.5	309	6.7	12.1	143	76	348	280	114	91	27
6-May-00	6333	50.83	2.355	13.22	12.14	0.18	7.65	10.80	2.16	0.397	0.226	99.95	24.0	304	6.8	11.9	140	90	372	272	113	89	26
6-Jun-00	6364	50.71	2.306	12.91	12.24	0.18	8.24	10.60	2.21	0.390	0.222	100.00	23.7	300	6.6	11.7	138	107	419	271	113	85	28
21-Jun-00	6379	51.01	2.361	13.33	12.04	0.18	7.23	10.88	2.31	0.405	0.228	99.98	24.4	308	6.6	12.2	143	80	354	282	113	88	29
14-Jul-00	6402	50.50	2.253	12.74	12.40	0.18	8.84	10.36	2.18	0.387	0.220	100.07	23.3	292	6.2	11.3	135	135	469	268	115	83	29
4-Aug-00	6423	50.77	2.288	12.93	12.28	0.18	8.29	10.56	2.17	0.390	0.224	100.10	23.9	299	6.4	11.7	138	112	416	276	113	93	28
12-Oct-00	6492	51.00	2.311	13.09	12.18	0.18	7.85	10.70	2.18	0.408	0.225	100.12	23.8	302	6.6	11.7	139	100	387	276	114	84	29
24-Dec-00	6565	50.75	2.348	13.21	12.04	0.18	7.39	10.75	2.48	0.402	0.229	99.78	24.4	308	6.7	12.1	143	87	355	280	114	87	29
8-Jan-01	6580	51.01	2.349	13.23	12.14	0.18	7.55	10.76	2.23	0.400	0.229	100.08	24.2	307	6.5	12.0	142	89	357	279	114	91	27
27-Jan-01	6599	50.69	2.360	13.30	12.16	0.18	7.56	10.79	2.22	0.402	0.260	99.91	24.3	308	6.5	12.1	139	87	357	283	113	94	29
16-Feb-01	6619	51.02	2.361	13.26	12.23	0.18	7.66	10.78	2.20	0.403	0.230	100.32	24.4	307	6.6	12.1	142	93	361	281	114	91	30
11-Mar-01	6642	50.83	2.369	13.25	12.21	0.18	7.53	10.76	2.25	0.405	0.229	100.01	24.4	310	6.8	12.0	144	93	346	284	115	93	28
8-Apr-01	6670	50.91	2.340	13.12	12.26	0.18	7.93	10.70	2.11	0.399	0.228	100.18	24.1	306	6.7	12.1	141	103	371	286	115	94	28
27-Apr-01	6689	50.61	2.371	13.26	12.17	0.18	7.53	10.81	2.18	0.404	0.227	99.73	24.2	308	6.3	11.9	139	91	376	277	112	95	28
24-May-01	6716	50.57	2.359	13.21	12.20	0.17	7.55	10.71	2.23	0.399	0.228	99.62	24.4	308	6.6	12.1	143	94	366	284	115	93	31
7-Jul-01	6760	50.20	2.340	13.19	12.15	0.17	7.36	10.66	2.89	0.400	0.230	99.59	24.5	310	6.7	12.3	144	91	357	287	114	91	33
15-Jul-01	6768	50.82	2.397	13.41	12.16	0.17	7.03	10.81	2.11	0.406	0.231	99.54	24.8	313	6.8	12.2	145	83	337	287	115	91	30
29-Sep-01	6844	51.19	2.454	13.69	12.20	0.18	6.69	10.95	2.13	0.418	0.236	100.14	24.8	319	6.7	12.6	148	69	283	283	114	88	32
13-Oct-01	6858	50.82	2.390	13.35	12.23	0.17	7.29	10.75	2.03	0.404	0.230	99.66	24.5	312	6.4	12.2	145	88	324	282	115	88	29
3-Nov-01	6879	50.81	2.384	13.34	12.21	0.17	7.25	10.74	1.98	0.401	0.230	99.52	24.3	312	6.6	12.1	145	83	332	280	120	90	29
12-Jan-02	6949	50.55	2.330	13.02	12.26	0.17	8.03	10.64	2.05	0.390	0.223	99.66	23.8	303	6.4	11.9	140	106	403	280	115	92	29
9-Feb-02	6977	50.79	2.338	13.11	12.31	0.17	7.90	10.68	2.03	0.391	0.224	99.94	24.2	305	6.4	11.8	140	103	376	276	115	90	29
27-Mar-02	7023	50.95	2.379	13.32	12.21	0.17	7.42	10.72	1.95	0.395	0.229	99.74	24.4	311	6.5	12.0	144	87	333	279	115	93	30
5-Apr-02	7032	50.84	2.340	13.21	12.20	0.17	7.79	10.71	2.05	0.389	0.225	99.92	24.1	306	6.3	11.9	141	94	379	275	114	94	28
12-Apr-02	7039	50.83	2.322	13.07	12.29	0.17	8.03	10.66	2.00	0.385	0.224	99.98	23.9	304	6.4	11.7	140	100	404	272	114	89	29
5-Jun-02	7093	50.88	2.340	13.19	12.29	0.18	7.96	10.66	2.13	0.394	0.227	100.25	24.3	305	6.4	11.7	141	99	379	277	115	91	30
16-Jun-02	7104	50.84	2.346	13.21	12.32	0.18	7.73	10.67	2.15	0.392	0.226	100.06	24.3	307	6.2	11.8	142	93	357	278	114	93	28
12-Jul-02	7130	50.90	2.407	13.47	12.19	0.18	7.09	10.80	2.19	0.406	0.234	99.87	25.0	315	6.6	12.2	146	79	328	280	115	92	32

(continued)

Table 3: *Continued*

Sample	Day	SiO <sub>2</sub>	TiO <sub>2</sub>	Al <sub>2</sub> O <sub>3</sub>	Fe <sub>2</sub> O <sub>3</sub> *	MnO	MgO	CaO	Na <sub>2</sub> O	K <sub>2</sub> O	P <sub>2</sub> O <sub>5</sub>	Total	Y	Sr	Rb	Nb	Zr	Ni	Cr	V	Zn	Ba	Ce
31-Jul-02	7149	50.92	2.374	13.34	12.25	0.18	7.46	10.70	2.06	0.396	0.230	99.91	24.7	312	6.5	12.0	144	87	343	280	116	92	33
6-Aug-02	7155	51.01	2.384	13.33	12.25	0.18	7.51	10.73	2.24	0.401	0.232	100.27	24.6	310	6.3	12.1	144	86	347	281	115	95	33
20-Aug-02	7169	50.82	2.337	13.09	12.37	0.18	8.11	10.62	2.15	0.390	0.225	100.29	24.2	306	6.5	11.8	142	103	374	273	115	97	29
27-Sep-02	7207	50.74	2.352	13.25	12.24	0.17	7.47	10.68	2.15	0.392	0.232	99.68	24.4	308	6.7	12.0	143	88	354	279	114	96	30
19-Oct-02	7229	50.96	2.381	13.33	12.20	0.18	7.13	10.75	2.15	0.394	0.238	99.71	24.5	311	6.8	12.2	144	79	351	285	114	92	30
21-Nov-02	7262	50.72	2.352	13.20	12.23	0.18	7.39	10.68	2.17	0.391	0.230	99.54	24.5	308	6.4	12.1	143	91	377	283	150	91	60
11-Jan-03	7313	50.76	2.372	13.36	12.17	0.18	7.29	10.73	2.22	0.394	0.231	99.69	24.7	311	6.8	12.1	144	82	348	285	115	91	29
11-Feb-03	7344	50.75	2.367	13.31	12.16	0.18	7.50	10.72	2.25	0.398	0.230	99.85	24.6	308	6.5	11.8	139	83	346	281	115	92	30
12-Mar-03	7373	50.78	2.354	13.21	12.23	0.18	7.62	10.66	2.19	0.392	0.229	99.84	24.5	308	6.9	12.0	143	91	357	279	115	95	30
12-Apr-03	7404	50.79	2.380	13.34	12.15	0.18	7.20	10.75	2.22	0.397	0.231	99.62	24.7	313	6.7	12.4	145	79	335	280	114	95	27
28-Jun-03	7481	50.73	2.376	13.42	12.14	0.18	7.08	10.78	2.30	0.401	0.234	99.63	24.8	315	6.8	12.4	145	77	321	286	115	103	26
31-Jul-03	7514	50.70	2.350	13.22	12.23	0.18	7.42	10.69	2.24	0.389	0.227	99.62	24.3	309	6.7	12.0	142	84	342	281	114	95	29
29-Aug-03	7543	50.87	2.385	13.43	12.19	0.18	7.08	10.77	2.34	0.401	0.235	99.86	24.7	312	6.6	12.4	145	78	336	286	115	101	28
19-Sep-03	7564	50.65	2.340	13.17	12.21	0.18	7.44	10.67	2.25	0.389	0.226	99.50	24.2	307	6.5	11.9	142	89	354	282	115	98	29
9-Oct-03	7584	50.87	2.379	13.27	12.15	0.18	7.45	10.78	2.25	0.398	0.231	99.94	24.7	311	6.6	12.0	141	82	346	285	114	98	28
15-Jan-04	7682	50.82	2.410	13.48	12.10	0.17	7.16	10.81	2.27	0.404	0.235	99.85	24.9	313	6.6	12.0	142	78	309	287	115	94	28
1-Mar-04	7728	50.83	2.415	13.38	12.11	0.18	7.20	10.86	2.27	0.405	0.235	99.88	24.9	314	6.7	12.2	144	79	309	288	114	92	31
16-Mar-04	7743	50.77	2.413	13.34	12.09	0.18	7.17	10.85	2.28	0.402	0.234	99.73	24.9	314	6.7	12.2	143	79	304	289	114	91	31
23-Apr-04	7781	50.83	2.418	13.45	12.23	0.18	7.13	10.85	2.28	0.408	0.236	100.00	24.9	314	6.6	12.2	143	77	293	282	112	93	30
2-Jun-04	7821	50.75	2.423	13.51	12.11	0.18	7.04	10.83	2.28	0.421	0.234	99.75	25.0	317	6.7	12.4	144	77	280	288	114	100	31
7-Jun-04	7826	50.92	2.436	13.56	12.12	0.18	6.99	10.82	2.30	0.417	0.239	99.98	25.2	318	6.6	12.3	144	75	262	286	114	97	32
23-Jul-04	7872	51.00	2.439	13.68	12.11	0.17	6.97	10.83	2.24	0.420	0.238	100.10	25.1	319	6.5	12.4	143	75	250	290	114	96	34
10-Aug-04	7890	50.71	2.361	13.33	12.04	0.17	7.46	10.90	2.31	0.405	0.225	99.91	24.2	309	6.2	11.9	137	87	351	280	112	94	30
15-Oct-04	7956	50.97	2.417	13.44	12.14	0.17	7.24	10.91	2.30	0.424	0.232	100.24	24.8	315	6.5	12.3	141	80	287	283	116	94	31
31-Oct-04	7972	50.85	2.448	13.51	12.14	0.18	6.90	10.85	2.39	0.424	0.234	99.93	25.2	319	6.7	12.5	144	75	243	294	116	100	31
4-Dec-04	8006	50.94	2.483	13.64	12.13	0.18	6.68	10.86	2.37	0.433	0.239	99.96	25.5	322	6.6	12.4	145	67	218	293	116	100	32
31-Jan-05	8064	50.98	2.492	13.63	12.23	0.18	6.69	10.85	2.44	0.425	0.239	100.16	25.5	320	6.5	12.5	144	69	217	288	115	100	32
6-Feb-05	8070	50.81	2.417	13.47	12.09	0.18	7.03	10.91	2.36	0.415	0.231	99.91	24.7	315	6.3	12.2	140	78	270	288	113	93	32
23-Feb-05	8087	50.80	2.437	13.52	12.13	0.18	6.98	10.86	2.42	0.418	0.232	99.98	25.1	317	6.5	12.4	141	77	255	289	114	94	34
4-Mar-05	8096	50.71	2.409	13.42	12.08	0.18	7.07	10.90	2.35	0.418	0.229	99.77	24.9	315	6.6	12.4	140	91	280	287	114	95	33
24-Mar-05	8116	50.79	2.395	13.42	12.12	0.17	7.28	10.92	2.35	0.408	0.230	100.08	25.5	315	6.5	12.7	146	86	298	289	115	100	32
22-Apr-05	8145	50.96	2.422	13.52	12.17	0.18	7.18	10.94	2.38	0.413	0.232	100.40	25.5	315	6.3	12.7	146	83	277	283	114	101	29
23-Jun-05	8207	50.76	2.451	13.58	12.14	0.17	6.85	10.83	2.54	0.417	0.235	99.97	25.9	319	6.5	13.0	150	77	247	291	116	104	30
16-Jul-05	8230	50.86	2.450	13.56	12.15	0.17	6.94	10.87	2.46	0.411	0.230	100.10	25.9	318	6.5	12.9	148	82	269	282	115	100	28
8-Aug-05	8253	50.89	2.430	13.52	12.05	0.18	6.91	10.79	2.50	0.415	0.230	99.92	26.0	318	6.5	13.0	148	79	259	291	116	102	32
23-Sep-05	8299	50.94	2.439	13.63	12.14	0.17	6.96	10.84	2.41	0.418	0.233	100.18	25.7	316	6.6	12.9	148	83	256	289	115	105	30
22-Oct-05	8328	50.85	2.437	13.62	12.12	0.17	6.98	10.80	2.42	0.413	0.229	100.04	25.8	315	6.9	12.9	147	82	255	290	115	104	28
19-Nov-05	8356	50.87	2.422	13.51	12.05	0.18	7.19	10.85	1.93	0.403	0.228	99.63	25.4	315	6.3	12.7	146	87	286	291	115	105	28
26-Dec-05	8393	50.84	2.432	13.47	12.07	0.18	7.09	10.83	2.06	0.405	0.231	99.61	25.8	315	6.1	12.6	147	86	276	291	116	97	29
<i>Hawaiian rock standards (Kilauea volcano)</i>																							
K1919 av.	—	49.88	2.797	13.63	12.04	0.17	6.63	11.39	2.38	0.548	0.292	99.75	—	—	—	—	—	—	—	—	—	—	
±2σ	—	0.24	0.03	0.19	0.07	0.007	0.24	0.04	0.32	0.012	0.006	—	—	—	—	—	—	—	—	—	—	—	
BHVO-1 av.	—	—	—	—	—	—	—	—	—	—	—	—	25.1	380	9.2	18.6	177	114	297	293	112	129	40
±2σ	—	—	—	—	—	—	—	—	—	—	—	—	0.3	7	0.5	0.4	8	2	3	6	2	8	2

\*Total iron given as Fe<sub>2</sub>O<sub>3</sub>.

Day is the number of days since the start of the Pu'u 'Ō'ō eruption on January 3, 1983. Oxide abundances are in wt %; trace element contents are in ppm. Samples 17-Jan-98, 11-May-98, and 7-Sep-98 are from Garcia *et al.* (2000). Between 1998 and 2005, K1919 (*n*=13) and BHVO-1 (*n*=13) were run as standards by XRF for major and trace element abundances, respectively.

Details of methods used and estimates of analytical precision for the XRF analyses have been given by Rhodes (1996) and Rhodes & Vollinger (2004).

In addition, 27 samples were analyzed over a 1 week period for Sc, V, Cr, Co, Ni, Cu, Zn, Sr, Cs, Rb, Ba, Th, U, Nb, Zr, Hf, Y, and rare earth element (REE) abundances using inductively coupled plasma mass spectrometry (ICP-MS) at the Australian National University (Table 4). The Kilauea rock standard BHVO-2 ( $n=2$ ) was analyzed with these samples. Analytical methods and estimates of precision for the ICP-MS trace element analyses are given in Table 4 and by Norman *et al.* (1998). Prior to both XRF and ICP-MS analyses, the Pu'u 'Ō'ō lava samples were washed in an ultrasonic bath of deionized water for 10–20 min, hand picked (30–100 g) to remove any rare altered rock chips, and powdered in a tungsten carbide swing mill for the XRF analyses and an agate mill for the ICP-MS analyses.

Fourteen Pu'u 'Ō'ō lavas erupted between 1998 and 2005 were analyzed for Pb and Nd isotope ratios (Table 5) by multi-collector (MC)-ICP-MS using a Nu Plasma system at San Diego State University (SDSU). Strontium isotope ratios were measured using this instrument and/or by thermal ionization mass spectrometry (TIMS) using a VG Sector 54 instrument at SDSU to compare the results of the two instruments. Additionally, four lavas erupted from 1989 to 1998 (Garcia *et al.*, 1992, 1996, 2000) were reanalyzed for Sr isotope ratios from the original dissolutions using TIMS to improve the analytical precision for these samples (Appendix, Table A1). A detailed overview of the analytical methods used in this study has been given by Marske *et al.* (2007). Additional details pertinent to this study are presented in Table 5.

## GEOCHEMISTRY OF 1998–2005 PU'U 'Ō'Ō LAVAS

The 1998–2005 Pu'u 'Ō'ō lavas are compositionally similar to earlier lavas from this eruption (Fig. 3). For example, their MgO contents (6.7–9.8 wt %) lie within the range of 1985–1998 lavas (6.7–10.1 wt %, excluding mixed and evolved lavas from episode 54). However, small, but significant short-term (years) variations in major element abundances (at a given MgO) are evident in these lavas (Fig. 3). Similar variations have been observed for historical Kilauea summit lavas and were related to changes in parental magma composition (e.g. Wright, 1971; Garcia *et al.*, 2003). Overall, Pu'u 'Ō'ō lavas have become progressively lower in CaO/Al<sub>2</sub>O<sub>3</sub> ratios and incompatible element (TiO<sub>2</sub> and K<sub>2</sub>O) contents, and higher in SiO<sub>2</sub> abundances (at a given MgO content) during the eruption (even if more differentiated samples with <7.2 wt % MgO are excluded; Fig. 3). At a given MgO content, the total variation of Fe<sub>2</sub>O<sub>3</sub><sup>\*</sup> (i.e. total iron), Al<sub>2</sub>O<sub>3</sub>, and Na<sub>2</sub>O abundances (not shown)

for the 1998–2005 lavas lie within the compositional field of previous lavas. The high SiO<sub>2</sub> and low CaO, TiO<sub>2</sub>, and K<sub>2</sub>O contents, and CaO/Al<sub>2</sub>O<sub>3</sub> ratios of the recent lavas expand the known compositional range for historical Kilauea lavas towards historical Mauna Loa lavas (Fig. 3).

The relatively low abundances and ratios of incompatible elements (e.g. Nb and La/Sm) in 1998–2005 lavas form trends that partially overlap with 1989–1997 Pu'u 'Ō'ō lavas, but also expand the compositional range to the lowest values observed during the eruption (Fig. 4). Recent Pu'u 'Ō'ō lavas continue the overall temporal decrease in highly to moderately incompatible trace element ratios (i.e. La/Yb) and abundances (i.e. Nb and Ba) since the early part of the eruption (Figs 4 and 5). These trace element abundances and ratios of the recent lavas, like the major element contents, extend the Pu'u 'Ō'ō compositional range toward the field of historical Mauna Loa lavas (Fig. 4).

The <sup>87</sup>Sr/<sup>86</sup>Sr ratios of the 1998–2005 lavas (0.70360–0.70364) are higher than those of previous Pu'u 'Ō'ō lavas (0.70357–0.70360). In contrast, Pb (Figs 5 and 6) and Nd isotope ratios are within the range of previous lavas. However, the 1998–2005 lavas make a small, yet distinctive trend in <sup>206</sup>Pb/<sup>204</sup>Pb vs <sup>87</sup>Sr/<sup>86</sup>Sr that expands the isotopic range for this eruption (Fig. 6). Unlike the major and trace element chemistry, these Pb and Sr isotope variations trend towards an area between the compositional fields of Kilauea and Mauna Loa (rather than directly towards the field of Mauna Loa lavas). Furthermore, this trend does not project towards a Hawaiian mantle end member (e.g. Kea or Loa) or towards the known isotopic composition of any other Hawaiian volcano.

## CRUSTAL MAGMATIC PROCESSES DURING THE ERUPTION

Olivine fractionation plays a dominant role in controlling the compositional variations in Hawaiian lavas (e.g. Powers, 1955; Wright, 1971). The importance of olivine crystallization in Pu'u 'Ō'ō lavas is evident from their wide range of MgO contents (5.6–10.1 wt %), and the presence of normally zoned olivine phenocrysts (Garcia *et al.*, 1996, 2000). Shallow magma mixing between stored rift magmas and 'fresh' MgO-rich magma(s) was an important process that controlled the composition of lavas erupted before February 1985 (episodes 1–29; Garcia *et al.*, 1992), and during episode 54 in January 1997 (Garcia *et al.*, 2000; Thornber *et al.*, 2003). Most (~93%) Pu'u 'Ō'ō lavas (excluding evolved lavas from episodes 1–29 and 54) have >7.2 wt % MgO, suggesting that the variation in the major element abundances of these lavas is primarily related to olivine fractionation and/or accumulation (i.e. olivine control; Wright, 1971). However, the MgO and Ni abundances of the Pu'u 'Ō'ō lavas have systematically decreased (with much scatter) since the eruption location

Table 4: ICP-MS analyses of 1998–2005 Pu`u `O`o lavas

Sample	Day	Rb	Cs	Ba	La	Ce	Pr	Nd	Sm	Eu	Gd	Tb	Dy	Ho	Er	Yb	Lu
17-Jan-98	5493	6.8	0.070	93.4	10.2	26.4	3.90	18.3	5.05	1.72	5.31	0.85	4.88	0.93	2.28	1.93	0.275
11-May-98	5607	7.0	0.072	95.8	10.3	26.8	3.96	18.5	5.10	1.71	5.36	0.85	4.90	0.93	2.31	1.95	0.273
7-Sep-98	5726	7.1	0.076	98.2	10.6	27.4	4.03	18.9	5.21	1.78	5.47	0.88	4.92	0.95	2.33	1.97	0.286
13-Feb-99	5885	7.3	0.073	99.4	10.7	27.7	4.09	19.1	5.26	1.80	5.62	0.89	5.07	0.97	2.38	2.02	0.288
19-Jun-99	6011	7.1	0.073	97.3	10.5	27.2	4.01	18.8	5.20	1.77	5.46	0.88	5.00	0.96	2.34	1.99	0.281
27-Oct-99	6141	6.9	0.070	96.8	10.5	27.1	3.99	18.8	5.11	1.77	5.52	0.88	4.95	0.96	2.34	2.00	0.278
19-Feb-00	6256	6.7	0.068	93.3	10.2	26.2	3.86	18.2	5.00	1.74	5.34	0.86	4.86	0.95	2.29	1.98	0.277
21-Jun-00	6379	6.7	0.065	93.9	10.2	26.2	3.83	18.3	4.97	1.73	5.43	0.87	4.90	0.95	2.31	2.00	0.278
12-Oct-00	6492	6.8	0.067	95.8	10.5	26.8	3.95	18.6	5.09	1.79	5.55	0.89	5.06	0.98	2.42	1.99	0.282
8-Jan-01	6580	6.9	0.070	95.9	10.5	26.7	3.97	18.7	5.10	1.78	5.53	0.88	5.03	0.98	2.38	2.03	0.283
8-Apr-01	6670	7.0	0.070	100	10.8	28.0	4.15	19.5	5.27	1.81	5.70	0.90	5.20	1.00	2.45	2.08	0.287
7-Jul-01	6760	6.9	0.069	98.4	10.6	27.6	4.07	19.1	5.20	1.79	5.65	0.89	5.07	0.99	2.43	2.03	0.284
13-Oct-01	6858	6.9	0.069	98.4	10.6	27.6	4.08	19.2	5.18	1.79	5.70	0.89	5.09	0.99	2.42	2.05	0.282
9-Feb-02	6977	6.6	0.067	93.1	10.1	26.1	3.86	18.1	4.95	1.71	5.39	0.85	4.86	0.95	2.29	1.94	0.273
5-Jun-02	7093	6.7	0.069	95.5	10.3	26.8	3.96	18.7	5.12	1.75	5.59	0.87	5.01	0.96	2.39	2.02	0.276
20-Aug-02	7169	6.7	0.070	95.9	10.3	26.8	3.96	18.7	5.15	1.79	5.48	0.89	5.08	0.98	2.41	2.02	0.286
21-Nov-02	7262	6.6	0.066	93.7	10.1	26.2	3.88	18.4	5.05	1.76	5.50	0.88	4.99	0.97	2.38	1.99	0.282
12-Apr-03	7404	6.9	0.071	98.0	10.6	27.4	4.04	19.1	5.28	1.83	5.68	0.90	5.21	1.01	2.46	2.07	0.290
19-Sep-03	7564	6.9	0.070	97.1	10.5	27.2	4.03	18.6	5.30	1.82	5.69	0.90	5.16	1.00	2.44	2.05	0.286
15-Jan-04	7682	7.1	0.073	99.3	10.7	27.8	4.10	19.4	5.31	1.86	5.69	0.92	5.22	1.02	2.51	2.10	0.293
23-Apr-04	7781	7.1	0.071	98.7	10.7	27.7	4.09	19.2	5.26	1.82	5.70	0.91	5.13	1.00	2.42	2.04	0.287
7-Jun-04	7826	7.4	0.078	103	11.2	29.0	4.28	20.0	5.47	1.89	6.00	0.94	5.37	1.04	2.52	2.14	0.300
15-Oct-04	7956	7.1	0.070	98.4	10.7	27.6	4.09	19.1	5.27	1.80	5.69	0.91	5.12	1.00	2.41	2.01	0.282
31-Jan-05	8064	7.5	0.076	104	11.2	29.0	4.30	20.1	5.55	1.89	5.92	0.95	5.31	1.05	2.50	2.13	0.294
22-Apr-05	8145	7.1	0.072	100	10.9	28.2	4.19	19.6	5.42	1.83	5.83	0.92	5.17	1.01	2.46	2.06	0.291
8-Aug-05	8253	7.2	0.073	102	11.0	28.4	4.18	19.8	5.46	1.85	5.87	0.93	5.30	1.01	2.49	2.09	0.295
14-Nov-05	8351	7.1	0.071	100	10.9	28.4	4.16	19.5	5.39	1.86	5.83	0.93	5.21	1.01	2.48	2.07	0.292
<i>Hawaiian rock standard (Kilauea volcano)</i>																	
BHVO-2	—	9.2	0.106	129	14.8	36.7	5.27	23.9	6.02	2.02	6.11	0.94	5.18	0.98	2.35	1.92	0.275
$\pm 2\sigma$	—	0.2	0.006	2.0	0.2	0.1	0.01	0.01	0.11	0.001	0.14	0.02	0.09	0.01	0.02	0.01	0.003

Sample	Day	Th	Y	Nb	Hf	U	Pb	Zr	Sr	Sc	V	Cr	Co	Ni	Cu	Zn	Ga
17-Jan-98	5493	0.81	23.8	12.0	3.42	0.260	1.01	139	313	30.8	264	432	52.6	171	120	105	18.9
11-May-98	5607	0.83	24.1	12.4	3.49	0.265	1.07	141	317	30.5	266	446	52.0	178	119	103	18.8
7-Sep-98	5726	0.84	24.3	12.6	3.55	0.278	1.04	143	322	30.8	268	449	49.3	149	120	103	18.9
13-Feb-99	5885	0.86	25.1	12.9	3.59	0.277	1.05	146	331	31.7	278	380	45.5	100	126	102	19.4
19-Jun-99	6011	0.84	24.9	12.7	3.59	0.271	1.04	145	327	31.4	277	440	50.5	137	122	104	19.2
27-Oct-99	6141	0.80	24.3	12.4	3.52	0.260	1.00	141	318	31.1	266	389	48.0	118	123	103	19.2
19-Feb-00	6256	0.80	23.8	12.1	3.44	0.259	1.07	138	309	30.7	261	418	50.3	133	121	106	18.8
21-Jun-00	6379	0.80	24.0	12.1	3.44	0.261	0.98	138	312	30.8	264	374	48.7	115	121	101	19.0
12-Oct-00	6492	0.81	24.7	12.3	3.52	0.261	1.04	142	318	31.9	268	364	47.8	103	123	109	19.5
8-Jan-01	6580	0.81	24.7	12.4	3.56	0.265	0.98	144	320	31.3	269	354	47.2	99	123	111	19.4
8-Apr-01	6670	0.85	25.1	12.6	3.65	0.282	1.00	144	325	31.4	270	302	45.4	89	124	104	19.9
7-Jul-01	6760	0.83	24.8	12.4	3.59	0.273	0.99	142	320	31.4	267	342	46.3	96	122	104	19.7
13-Oct-01	6858	0.83	24.7	12.4	3.58	0.264	0.97	142	320	31.3	266	347	47.2	105	121	105	19.6
9-Feb-02	6977	0.78	23.7	11.7	3.40	0.261	0.93	135	306	30.6	256	417	51.5	140	114	102	18.6

(continued)

Table 4: Continued

Sample	Day	Th	Y	Nb	Hf	U	Pb	Zr	Sr	Sc	V	Cr	Co	Ni	Cu	Zn	Ga
5-Jun-02	7093	0.80	24.4	12.1	3.50	0.266	0.96	139	315	30.6	262	347	47.5	108	117	101	19.1
20-Aug-02	7169	0.78	24.3	12.2	3.54	0.269	0.95	139	314	30.4	260	325	47.7	108	119	103	19.2
21-Nov-02	7262	0.78	24.1	11.9	3.48	0.257	0.93	137	309	31.0	260	409	48.2	114	116	104	18.9
12-Apr-03	7404	0.81	25.0	12.4	3.62	0.270	0.98	143	322	31.2	267	306	44.7	82	122	103	19.7
19-Sep-03	7564	0.81	25.1	12.4	3.56	0.271	0.97	143	322	31.5	268	341	47.9	98	124	107	19.9
15-Jan-04	7682	0.83	25.2	12.6	3.67	0.268	1.00	145	326	31.1	270	287	44.5	83	120	102	19.6
23-Apr-04	7781	0.83	25.2	12.7	3.61	0.267	1.00	146	327	31.6	271	297	45.8	91	122	105	19.9
7-Jun-04	7826	0.87	26.3	13.3	3.77	0.284	1.02	153	341	32.4	281	261	46.0	85	127	108	20.7
15-Oct-04	7956	0.83	25.1	12.7	3.61	0.275	1.01	145	327	31.7	272	304	45.0	90	120	104	19.9
31-Jan-05	8064	0.88	26.2	13.4	3.78	0.279	1.06	153	342	32.0	281	214	44.3	77	126	107	20.4
22-Apr-05	8145	0.86	25.2	12.9	3.68	0.278	1.02	147	329	31.8	273	267	46.0	93	123	107	20.1
8-Aug-05	8253	0.84	25.5	12.8	3.65	0.281	1.01	147	331	31.8	273	255	45.1	89	124	106	20.2
14-Nov-05	8351	0.85	25.2	12.7	3.64	0.273	0.89	146	331	31.8	271	—	45.4	94	122	105	20.1
<i>Hawaiian rock standard (Kilauea volcano)</i>																	
BHVO-2 av.	—	1.25	24.4	18.0	4.17	0.408	1.68	169	388	31.2	278	282	42.9	115	121	99	20.0
$\pm 2\sigma$	—	0.02	0.5	0.6	0.04	0.008	0.04	3	9	1.0	9	10	2.2	6	6	4	0.5

Day is the number of days since the start of the Pu'u 'Ō'ō eruption on January 3, 1983; values are in ppm. BHVO-2 ( $n=2$ ) was analyzed as an internal standard for these analyses.

shifted in early 1992 from the Kūpaianaha vent to the Pu'u 'Ō'ō cone (Figs 3 and 5), suggesting that Pu'u 'Ō'ō magmas are becoming increasingly differentiated with time. Clinopyroxene fractionation has become an increasingly important process for 1998–2005 lavas. For example, there is a greater abundance of clinopyroxene microphenocrysts in the 1998–2005 lavas (up to 3 vol. %; Table 1) compared with earlier erupted Pu'u 'Ō'ō lavas (<1 vol. % or absent), and ~50% of the most recent lavas (2004–2005) have differentiated beyond olivine control (<7.2 wt % MgO; Fig. 5).

Olivine accumulation has also affected some Pu'u 'Ō'ō lava compositions based on the low Fo contents of some olivines compared with their whole-rock Mg-number (Fig. 2). For example, the maximum MgO difference for two olivine-controlled 1998–2005 lavas (23-Jul-04, 7.0 wt % MgO; 4-Jan-00, 9.5 wt % MgO) with similar olivine Fo contents (81–82%; Fig. 2) can be explained by the accumulation of ~6.1 vol. % olivine. This is consistent with the 5% greater modal abundance of olivine phenocrysts in sample 4-Jan-00 compared with 23-Jul-04, and the position of sample 4-Jan-00 to the right of the equilibrium field in Fig. 2. All of the 2003–2005 lavas analyzed have Fo contents in equilibrium with their bulk compositions (Fig. 2).

## TEMPORAL COMPOSITIONAL VARIATIONS

Pu'u 'Ō'ō lavas display systematic temporal variations of MgO-normalized major element abundances, ratios of

highly to moderately incompatible trace elements (e.g. La/Yb), highly incompatible trace element ratios (e.g. Ba/Nb), and Pb and Sr isotope ratios (Fig. 5). At least three distinct end-member magma compositions may be delineated based on correlated temporal changes among some MgO-normalized major element abundances, and incompatible trace element and Sr isotope ratios: (1) 1985–1998 (days ~760–5500); (2) 1998–2003 (days ~5501–7400); (3) 2003–2005 (days ~7401–8400). Magma mixing affected the composition of lavas erupted before February 1985 (days 1–745; Garcia *et al.*, 1992) and during episode 54 in January 1997 (day 5141; Garcia *et al.*, 2000; Thornber *et al.*, 2003), and these lavas were excluded from the plots.

The SiO<sub>2</sub> temporal trend for Pu'u 'Ō'ō lavas inversely correlates with the temporal variations of CaO and TiO<sub>2</sub> (Fig. 5). Between ~1985 and 1998, MgO-normalized major element abundances display relatively flat (SiO<sub>2</sub>) and slightly decreasing (CaO and TiO<sub>2</sub>) trends. However, lavas erupted between ~1998 and 2003 display changes in slope with significant increases and decreases in these abundances, respectively, until mid-2003 (Fig. 5). Following a compositional reversal in mid-2003, the MgO-normalized SiO<sub>2</sub> abundances have decreased whereas CaO and TiO<sub>2</sub> contents have increased. In contrast, Al<sub>2</sub>O<sub>3</sub> and Fe<sub>2</sub>O<sub>3</sub> contents (not shown) have remained nearly constant.

Pu'u 'Ō'ō lavas also display systematic fluctuations in incompatible trace element ratios that correlate with the major element changes (Fig. 5). Between ~1985 and 1998

Table 5: Pb, Sr and Nd isotope data for Pu'u 'Ō'ō lavas

Sample	$^{206}\text{Pb}/^{204}\text{Pb}$	$^{207}\text{Pb}/^{204}\text{Pb}$	$^{208}\text{Pb}/^{204}\text{Pb}$	$^{87}\text{Sr}/^{86}\text{Sr}$	$^{143}\text{Nd}/^{144}\text{Nd}$	$\varepsilon_{\text{Nd}}$
7-Sep-98	18.4107	15.4727	38.0752	$0.703601 \pm 6$	0.512956	+6.21
13-Feb-99	18.4124	15.4736	38.0764	$0.703616 \pm 6$	0.512944	+5.97
27-Oct-99	18.4018	15.4726	38.0687	$0.703622 \pm 9$	0.512948	+6.04
19-Feb-00	18.4072	15.4712	38.0720	$0.703634 \pm 7$	0.512944	+5.97
21-Jun-00	18.4067	15.4704	38.0688	$0.703644 \pm 7$	0.512947	+6.04
8-Jan-01	18.4116	15.4721	38.0737	$0.703639 \pm 12$	0.512946	+6.01
7-Jul-01	18.4137	15.4719	38.0729	$0.703626 \pm 9$	0.512943	+5.95
9-Feb-02	18.4139	15.4707	38.0691	$0.703637 \pm 8$	0.512940	+5.89
20-Aug-02	18.4152	15.4722	38.0719	$0.703639 \pm 5$	0.512945	+5.98
12-Apr-03	18.4161	15.4726	38.0715	$0.703641 \pm 5$	0.512953	+6.14
15-Jan-04	18.4154	15.4719	38.0694	$0.703632 \pm 7$	0.512946	+6.01
7-Jun-04	18.4146	15.4716	38.0680	$0.703623 \pm 7$	0.512943	+5.95
31-Jan-05	18.4170	15.4735	38.0752	$0.703624 \pm 5$	0.512955	+6.19
8-Aug-05	18.4119	15.4727	38.0699	$0.703622 \pm 10$	0.512953	+6.14
<i>Hawaiian rock standard (Kilauea volcano)</i>						
Kil1919	18.6562	15.4903	38.2092	0.703477	0.512973	+6.53

The Pb, Sr and Nd isotope ratios of the samples were measured over two periods of time. The 1998–2004 Pu'u 'Ō'ō lavas were analyzed at the same time as the Kilauea samples presented by Marske *et al.* (2007), whereas the 2005 lavas, a new dissolution of Kil1919 (a Hawaiian rock standard collected from the same flow as K1919, BHVO-1, and BHVO-2) and the reanalyzed 1989–1995 lavas in Table A1 in the Appendix [previously studied by Garcia *et al.* (1996, 2000) and Pietruszka *et al.* (2006)] were analyzed subsequently by MC-ICP-MS (for Pb and Nd isotopes) and TIMS (for Sr isotopes). Analytical details relevant to the 1998–2004 samples have been presented by Marske *et al.* (2007). The following analytical details apply to the other samples, unless otherwise noted. Pb isotope ratios were corrected for instrumental mass fractionation using the measured isotope ratio of Tl (SRM997) added to the sample compared with an assumed  $^{205}\text{Tl}/^{203}\text{Tl} = 2.3889$  for this standard from Thirlwall (2002). The average Tl-corrected value for NBS981 Pb ( $n=5$ ) was  $^{206}\text{Pb}/^{204}\text{Pb} = 16.9434 \pm 15$  ( $2\sigma$ ),  $^{207}\text{Pb}/^{204}\text{Pb} = 15.5019 \pm 16$  ( $2\sigma$ ), and  $^{208}\text{Pb}/^{204}\text{Pb} = 36.7298 \pm 42$  ( $2\sigma$ ). All of the Pb isotopic data are reported relative to the NBS981 Pb standard values of Galer & Abouchami (1998):  $^{206}\text{Pb}/^{204}\text{Pb} = 16.9405$ ,  $^{207}\text{Pb}/^{204}\text{Pb} = 15.4963$ , and  $^{208}\text{Pb}/^{204}\text{Pb} = 36.7219$ . Sr and Nd isotope ratios were corrected for instrumental mass fractionation relative to  $^{86}\text{Sr}/^{88}\text{Sr} = 0.1194$  and  $^{146}\text{Nd}/^{144}\text{Nd} = 0.7219$ , respectively. The average measured values for Sr and Nd standards were  $^{87}\text{Sr}/^{86}\text{Sr} = 0.710246 \pm 17$  ( $2\sigma$ ;  $n=18$ ) for SRM987 (by TIMS) and  $^{143}\text{Nd}/^{144}\text{Nd} = 0.512103 \pm 7$  ( $2\sigma$ ;  $n=6$ ) for Ames Nd (by MC-ICP-MS). All Sr and Nd isotopic data are reported relative to constant standard values for SRM987 ( $^{87}\text{Sr}/^{86}\text{Sr} = 0.710250$ ) and Ames Nd ( $^{143}\text{Nd}/^{144}\text{Nd} = 0.512130$ ). After correcting to this value for Ames Nd, a single analysis of the La Jolla Nd standard as an unknown gave  $^{143}\text{Nd}/^{144}\text{Nd} = 0.511845$ . The estimated reproducibility ( $\pm 2\sigma$ ) for all of the data is based on multiple analyses of the La Jolla Nd standard and the Kil1919 rock standard by Marske *et al.* (2007). Uncertainties of the single Sr analyses are based on the  $\pm 2\sigma_m$  ( $n>4$ ) of replicate analyses of each sample reported in Table A1 and by Garcia *et al.* (1996, 2000) and Pietruszka *et al.* (2006). Total procedural blanks were negligible compared with the amount of sample used ( $>0.6\text{ g}$ ) and the concentrations of Pb, Sr, and Nd in the samples.

there are small but significant decreases in some ratios of incompatible trace elements until day  $\sim 5500$ . Between  $\sim 1998$  and 2003 these incompatible trace element ratios display flattening (e.g. La/Yb) or nearly constant (e.g. Ba/Nb) temporal trends. Some ratios of highly over moderately incompatible trace elements (e.g. La/Yb) record a small compositional reversal in mid-2003, followed by a small increase similar to the reversal recorded by the normalized major element abundances (Fig. 5).

The  $^{87}\text{Sr}/^{86}\text{Sr}$  ratios of Pu'u 'Ō'ō lavas gradually increased between  $\sim 1985$  and 1998, before a sharper increase occurred in 1998 (day  $\sim 5500$ ). This shift coincided with the significant increases in MgO-normalized  $\text{SiO}_2$  abundances and decreases in the CaO and  $\text{TiO}_2$

abundances (Fig. 5). The  $^{87}\text{Sr}/^{86}\text{Sr}$  ratios increased to the highest observed values for this eruption in mid-2003, and reversed from 2003 to 2005. This is also analogous to the reversals of MgO-normalized major element abundances and incompatible trace element ratios (Fig. 5). In contrast, the Pb and Nd isotope ratios have remained relatively constant since 1985 (relative to analytical error), especially for the 1998–2005 lavas (Fig. 5; Table 5).

In summary, three distinct end-member compositions are important during the Pu'u 'Ō'ō eruption. First, an early end member ( $\sim 1985$ ) has relatively low  $^{87}\text{Sr}/^{86}\text{Sr}$  ratios and MgO-normalized  $\text{SiO}_2$  abundances, and high CaO and  $\text{TiO}_2$  abundances and incompatible trace element ratios (e.g. Ba/Nb or La/Yb). Second, a later end

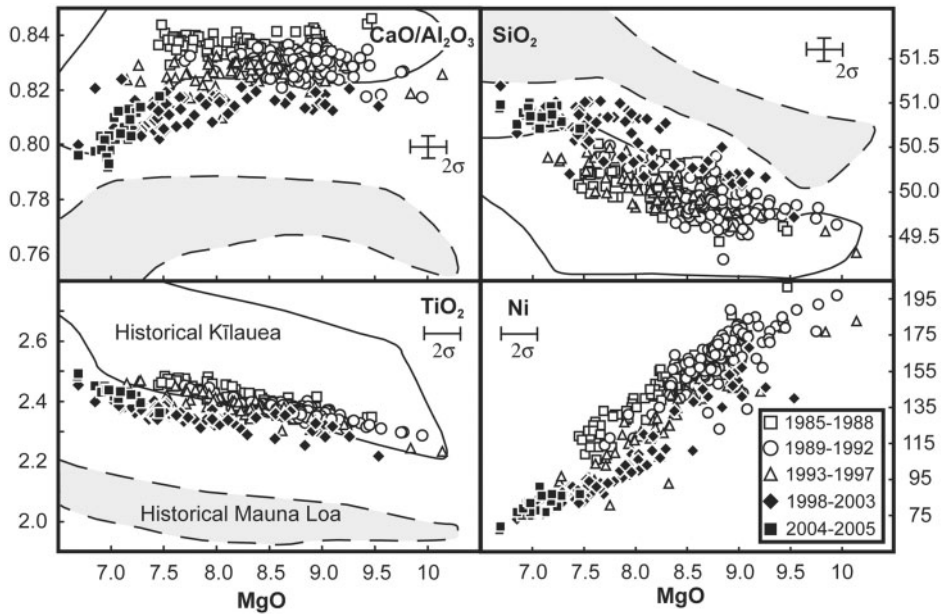


**Fig. 3.** Whole-rock  $MgO$  variation diagrams for Pu'u 'O'o lavas, historical Kīlauea (Garcia *et al.*, 2003), and historical Mauna Loa (Rhodes & Hart, 1995) lavas. The Pu'u 'O'o lavas are grouped according to eruption date (see inset for symbols). The new 1998–2005 Pu'u 'O'o data (filled symbols) from Table 3 are plotted with previous data (open symbols) from Garcia *et al.* (1992, 1996, 2000). These groups were further subdivided to better resolve the systematic geochemical changes, and to emphasize the rapid temporal changes during the eruption. Mixed and/or evolved Pu'u 'O'o lavas (episodes 1–29 and 54) are not shown in this and subsequent figures. All values are in wt % (except  $CaO/Al_2O_3$ ). The  $2\sigma$  error bars are shown in the corner of each plot unless they are smaller than the size of the symbols.

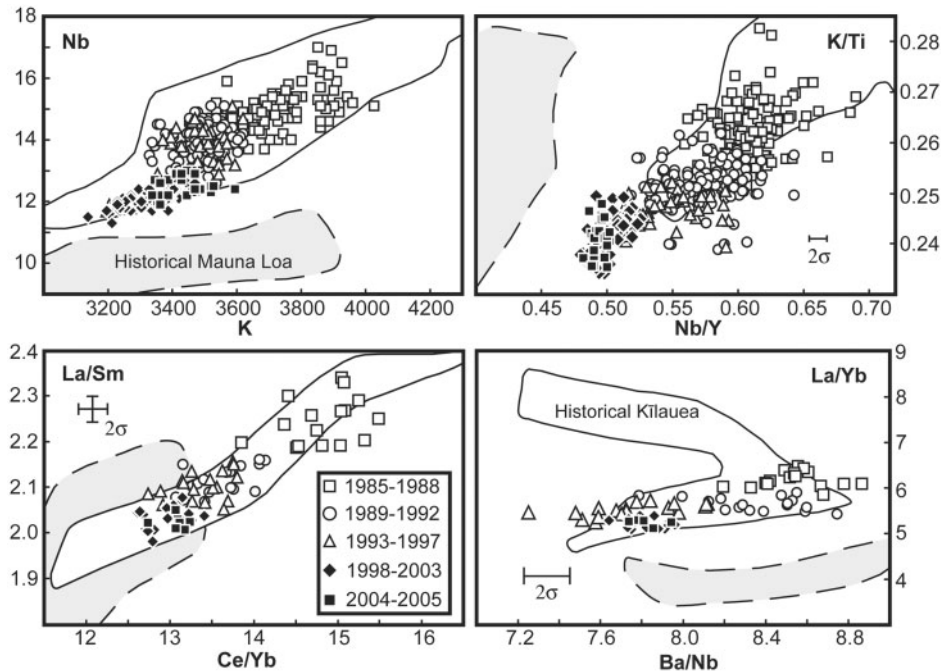


**Fig. 4.** Incompatible trace element abundance and ratio–ratio variation diagrams for Pu'u 'O'o lavas. The compositional fields of historical Kīlauea (Pietruszka & Garcia, 1999a; Garcia *et al.*, 2003) and Mauna Loa (Rhodes & Hart, 1995; J. M. Rhodes, unpublished data, 2008) lavas are also plotted. The  $2\sigma$  error bars are shown in the corner of each plot unless they are smaller than the size of the symbols. The values are in ppm except for the ratios. Estimates for the analytical precision of Pu'u 'O'o lavas analyzed (by ICP-MS) prior to this study have been given by Garcia *et al.* (1996, 2000). The Kīlauea rock standards Kill199 and BHVO-2 come from the same lava flow. Pu'u 'O'o ICP-MS trace element data from previous studies were corrected by normalizing the average Kill199 standard ( $n=11$ ) used for 1985–1998 Pu'u 'O'o lavas to the BHVO-2 standard values for this study. Although the Kill199 and BHVO-2 standards differ by 0.3 wt %  $MgO$ , if this was due to olivine control (as expected) the maximum difference in the incompatible trace element concentrations would be 0.7%, which is within analytical uncertainty of the ICP-MS data (Norman *et al.*, 1998).

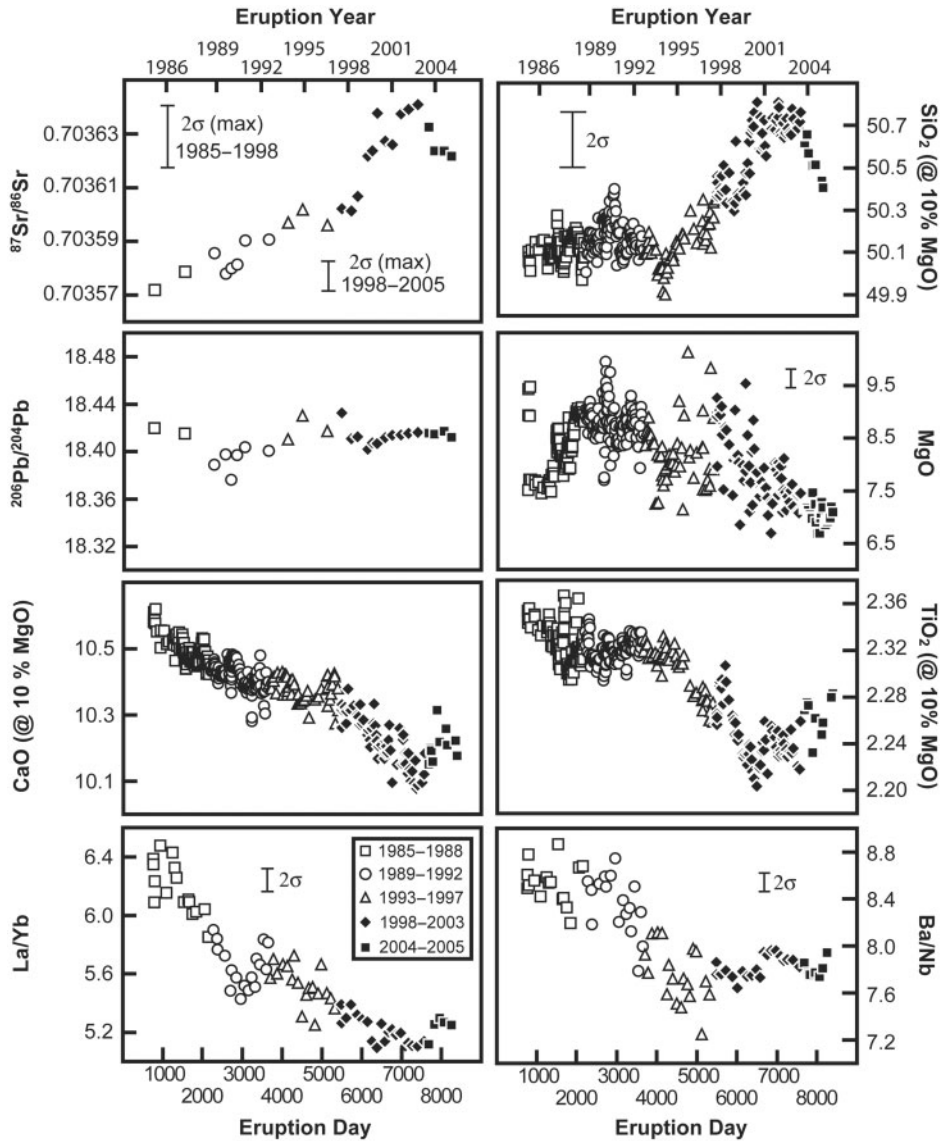


**Fig. 5.** Temporal geochemical variations during the Pu'u 'Ō'ō eruption. The 1985–1998 Pu'u 'Ō'ō lava data are from Garcia *et al.* (1992, 1996, 2000).  $\text{SiO}_2$ ,  $\text{CaO}$ , and  $\text{TiO}_2$  were normalized to 10 wt %  $\text{MgO}$  (the most primitive lava erupted from Pu'u 'Ō'ō; Garcia *et al.*, 2000) by the addition of equilibrium composition olivine (98.5%) and spinel (1.5%) in 0.5 mol % steps (Garcia *et al.*, 2003; Rhodes & Vollinger, 2005). Pu'u 'Ō'ō lavas with <7.2 wt %  $\text{MgO}$  may have crystallized minerals other than olivine (e.g. clinopyroxene and plagioclase) and were not included in the olivine normalization procedure. The decrease in scatter for the  $^{206}\text{Pb}/^{204}\text{Pb}$ ,  $\text{Ba}/\text{Nb}$ , and  $\text{La}/\text{Yb}$  ratios after 1998 is attributed to higher precision for the more recent trace element and Pb isotopic data. The  $2\sigma$  error bars are shown in the corner of each plot unless they are smaller than the size of the symbols. The maximum  $2\sigma$  error bars are presented in the Sr isotope panel for lavas erupted between 1985 and 1998 and between 1998 and 2005. The  $^{87}\text{Sr}/^{86}\text{Sr}$  analytical uncertainties for each sample (presented in Table 5) are typically smaller than the maximum  $2\sigma$  error bar.

member ( $\sim 1998$ ) from a recently depleted source (Pietruszka *et al.*, 2006) has slightly higher  $^{87}\text{Sr}/^{86}\text{Sr}$  and  $\text{MgO}$ -normalized  $\text{SiO}_2$  contents, yet lower incompatible trace element ratios and  $\text{CaO}$  and  $\text{TiO}_2$  abundances. Third, the most recent end-member composition ( $\sim 2003$ ) displays the highest  $^{87}\text{Sr}/^{86}\text{Sr}$  ratios and  $\text{MgO}$ -normalized  $\text{SiO}_2$  abundances, and lowest abundances of  $\text{CaO}$  and  $\text{TiO}_2$  and ratios of incompatible trace elements for the eruption.

## PU'U 'Ō'ō SOURCE CHARACTERISTICS A lithospheric source component for Pu'u 'Ō'ō lavas?

Magmas originating from partial melting within the Hawaiian plume can be compositionally modified at shallower depths by the assimilation of hydrothermally altered oceanic crust (e.g. Eiler *et al.*, 1996) or lower gabbroic crust

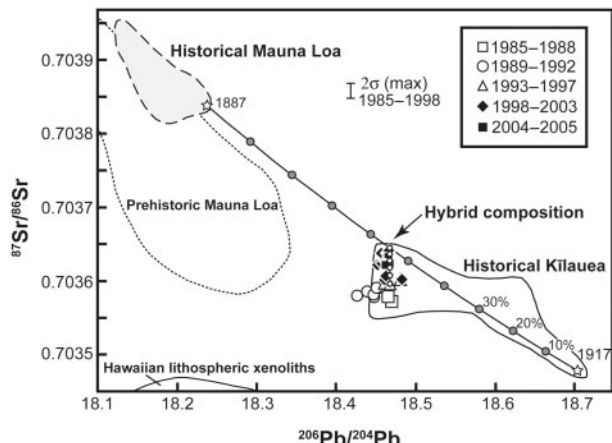


**Fig. 6.**  $^{206}\text{Pb}/^{204}\text{Pb}$  vs  $^{87}\text{Sr}/^{86}\text{Sr}$  isotope ratios for Pu'u 'Ō'ō lavas compared with historical Kīlauea, and prehistoric and historical Mauna Loa lavas. Data sources: Garcia *et al.* (1992, 1996, 2000) for 1985–1998 Pu'u 'Ō'ō lavas; Pietruszka & Garcia (1999a) and Abouchami *et al.* (2005) for historical Kīlauea lavas; Kurz & Kammer (1991), Kurz *et al.* (1995), Rhodes & Hart (1995), Warless *et al.* (2006), and Marske *et al.* (2007) for historical and prehistoric Mauna Loa lavas. The compositional fields of Pacific mid-oceanic ridge basalts ( $^{206}\text{Pb}/^{204}\text{Pb} = 18.24\text{--}19.48$  and  $^{87}\text{Sr}/^{86}\text{Sr} = 0.70264\text{--}0.70367$ ; King *et al.*, 1993; Fekiacova *et al.*, 2007) and most Hawaiian lithospheric xenoliths ( $^{206}\text{Pb}/^{204}\text{Pb} = 17.58\text{--}18.38$  and  $^{87}\text{Sr}/^{86}\text{Sr} = 0.70271\text{--}0.70347$ ; Okano & Tatsumoto, 1996; Lassiter & Hauri, 1998) lie off the figure (below the isotopic fields of Kīlauea and Mauna Loa). Mixing lines between AD 1917 Kīlauea and AD 1887 Mauna Loa lavas (line with gray circles) and between a Pu'u 'Ō'ō sample (10-Jan-1997) and a hybrid source (line with small open circles) containing a 55:45 proportion of the historical Kīlauea and Mauna Loa compositions are shown. The Pb abundances assumed for the mixing model are 1 ppm for Kīl1917 ( $^{206}\text{Pb}/^{204}\text{Pb} = 18.653$ ,  $^{87}\text{Sr}/^{86}\text{Sr} = 0.703478$ ) and 10-Jan-1997 ( $^{206}\text{Pb}/^{204}\text{Pb} = 18.417$ ,  $^{87}\text{Sr}/^{86}\text{Sr} = 0.703596$ ) based on the average Pb concentrations in Table 4, and 0.9 ppm Pb for the 1887 Mauna Loa ( $^{206}\text{Pb}/^{204}\text{Pb} = 18.487$ ,  $^{87}\text{Sr}/^{86}\text{Sr} = 0.703838$ ) lava. The Sr concentrations in the mixing end members are from Pietruszka & Garcia (1999a) for the 1917 Kīlauea lava (389 ppm Sr), Rhodes & Hart (1995) for 1887 Mauna Loa lava (275 ppm Sr), and Garcia *et al.* (2000) for the 10-Jan-1997 lava (307 ppm Sr). The maximum  $2\sigma$  error bars are presented for 1985–1998 lavas. The  $2\sigma$  error bars for 1998–2005 Pb and Sr isotope ratios are smaller than the size of the symbol.

(e.g. Gaffney *et al.*, 2004), or by partial melting of the upper ambient mantle (lithosphere or asthenosphere) beneath Hawai'i (e.g. Tatsumoto, 1978; Chen & Frey, 1985; Stille *et al.*, 1986; Lassiter *et al.*, 1996). However, it is unlikely that crustal assimilation or melting of the upper ambient mantle significantly modified the chemical signature of Pu'u 'Ō'ō lavas. Pu'u 'Ō'ō lavas erupted between 1983 and 1986 have relatively low  $\delta^{18}\text{O}$  groundmass values (4.6–5.0‰) that are in disequilibrium with their olivine phenocrysts, suggesting that these early magmas interacted with shallow wall rock in the rift zone just prior to eruption (Garcia *et al.*, 1998). The switch in eruptive style from episodic lava fountaining to near-continuous effusion in 1986 led to a marked reduction or elimination of contamination, based on higher  $\delta^{18}\text{O}$  groundmass values (5.0–5.3‰) in equilibrium with olivines in the 1986–1998

lavas (Garcia *et al.*, 1998). Furthermore, the 1998–2003 Pu'u 'Ō'ō lavas record systematic temporal increases in  $^{87}\text{Sr}/^{86}\text{Sr}$  ratios and relatively constant  $^{206}\text{Pb}/^{204}\text{Pb}$  ratios (Fig. 6) that trend away from the compositional fields of lithospheric mantle xenoliths from Salt Lake Crater, O'ahu (Okano & Tatsumoto, 1996) and Hualālai volcano, Hawai'i (Lassiter & Hauri, 1998), and Cretaceous Pacific mid-oceanic ridge basalts near Hawai'i (e.g. Ocean Drilling Program Site 843; King *et al.*, 1993; Fekiacova *et al.*, 2007).

Historical Kīlauea summit lavas have relatively low  $\delta^{18}\text{O}$  isotope values that are attributed to <5–12% contamination of parental magmas with altered country rock from both Kīlauea and Mauna Loa (Garcia *et al.*, 2008). The overall increase of Sr isotopes in Pu'u 'Ō'ō lavas could potentially be explained if a more typical Kīlauea parental magma (e.g. 1993–1997 Pu'u 'Ō'ō lavas) progressively assimilated a roughly constant (55:45) mixture of older Kīlauea and Mauna Loa basement rocks (Fig. 6). However, this would require ~100% contamination because the Pu'u 'Ō'ō lava with the highest  $^{87}\text{Sr}/^{86}\text{Sr}$  ratio overlaps with the composition of the 55:45 Kīlauea–Mauna Loa assimilant. These combined observations suggest that melt interaction with the upper mantle, crust, or volcanic edifice beneath Kīlauea is minimal for recent Pu'u 'Ō'ō lavas.

### A third mantle source for the Pu'u 'Ō'ō eruption

At least three distinct mantle source components are required to explain the compositional variability of Pu'u 'Ō'ō lavas (Fig. 7). The 1985–1998 Pu'u 'Ō'ō lavas originated from at least two distinct source components with similar Kīlauea-like Pb, Sr, and Nd isotopic compositions but different incompatible element abundances and ratios (Garcia *et al.*, 2000). One component with higher MgO-normalized CaO and TiO<sub>2</sub> abundances and incompatible trace element ratios (e.g. Ba/Ce or La/Yb) was important during the early part of the eruption (~1985; Figs 5 and 7), following the period of magma mixing during episodes 1–29. The temporal decreases among  $^{230}\text{Th}$ – $^{238}\text{U}$  and  $^{226}\text{Ra}$ – $^{230}\text{Th}$  disequilibria, incompatible trace element ratios (e.g. Th/U or Nd/Sm), and some normalized major element abundances in lavas from 1985 to 2001 (Fig. 5) suggest that a second mantle component was tapped (Pietruszka *et al.*, 2006). This 'recently depleted' component is thought to have formed at <8 ka (based on modeling of  $^{226}\text{Ra}$ – $^{230}\text{Th}$ – $^{238}\text{U}$  disequilibria) by the removal of melt from Kīlauea's source region within the Hawaiian plume, causing it to become depleted in incompatible trace elements (Pietruszka *et al.*, 2006). A progressive increase in the proportion of the recently depleted component is indicated by the temporal trends between 1985 and 1998 (Figs 5 and 7; Garcia *et al.*, 2000; Pietruszka *et al.*, 2006).

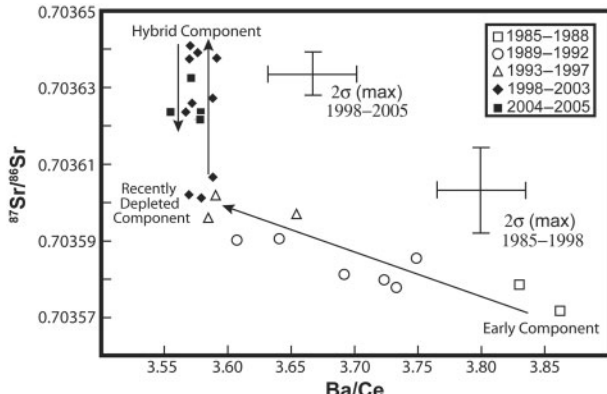


**Fig. 7.** Ba/Ce vs  $^{87}\text{Sr}/^{86}\text{Sr}$  for Pu'u 'O'o lavas. The 1985–1998 Pu'u 'O'o lava data are from Garcia *et al.* (1992, 1996, 2000). At least three distinct mantle sources (termed the early, recently depleted and hybrid components) are required to explain the chemical variability during the Pu'u 'O'o eruption. The maximum  $2\sigma$  error bar is presented for 1985–1998 and 1998–2005 lavas (Sr isotopes only). Historical Mauna Loa lavas display a lower Ba/Ce range (2.6–3.5; J. M. Rhodes, unpublished data, 2008), with higher Sr isotope values ( $>0.70375$ ; Rhodes & Hart, 1995).

The systematic geochemical variations from 1998 to 2003 (Figs 5–7) require a third component that was increasingly tapped during this time interval. Based on the temporal increases of some highly incompatible trace element ratios (e.g. Ba/Th) in lavas erupted from 1999 to 2001, Pietruszka *et al.* (2006) suggested that Pu'u 'O'o lavas are derived in greater proportions of a source component similar to historical Mauna Loa lavas. However, simple mixing of melt from a Mauna Loa-like source (with relatively low  $^{206}\text{Pb}/^{204}\text{Pb}$  and high  $^{87}\text{Sr}/^{86}\text{Sr}$ ) with an earlier Pu'u 'O'o composition (i.e. the recently depleted component) cannot explain the increase in  $^{87}\text{Sr}/^{86}\text{Sr}$  ratios at relatively constant  $^{206}\text{Pb}/^{204}\text{Pb}$  ratios between 1998 and 2003 (Fig. 6).

Rhodes *et al.* (1989) proposed that magma from Mauna Loa may periodically invade Kilauea's plumbing system. Pre-mixing of nearly equal proportions of historical Kilauea- and Mauna Loa-like magmas prior to eruption could potentially explain the trends of recent Pu'u 'O'o lavas (Figs 6 and 8). Although this pre-mixing could occur in Kilauea's  $\sim 2\text{--}3 \text{ km}^3$  summit reservoir (Pietruszka & Garcia, 1999b), the rapid compositional

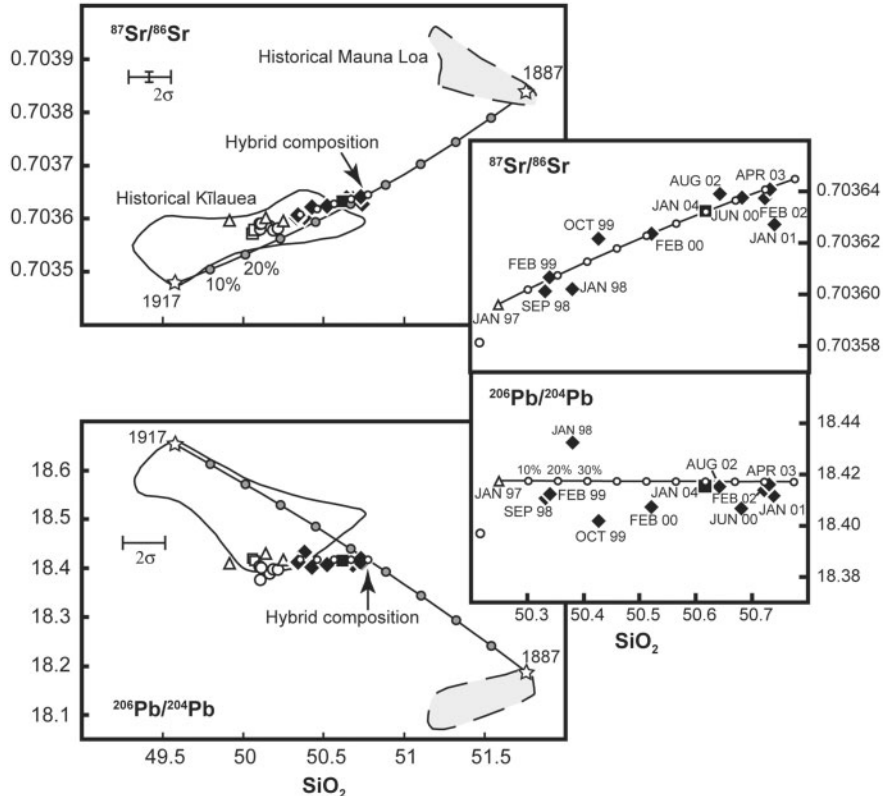


**Fig. 8.**  $^{206}\text{Pb}/^{204}\text{Pb}$  and  $^{87}\text{Sr}/^{86}\text{Sr}$  vs  $\text{MgO}$ -normalized  $\text{SiO}_2$  abundances for Pu'u 'O'o and historical Kilauea and Mauna Loa lavas. Data sources: Garcia *et al.* (1992, 1996, 2000) for 1985–1998 Pu'u 'O'o lavas; Pietruszka & Garcia (1999a), Garcia *et al.* (2003), and Abouchami *et al.* (2005) for historical Kilauea lavas; Rhodes & Hart (1995) for historical Mauna Loa lavas. Mixing lines between a Pu'u 'O'o sample (10-Jan-1997) and a hybrid composition containing a 55:45 proportion of historical Kilauea (i.e. AD 1917) and Mauna Loa (i.e. AD 1887) compositions are shown. Mixing model details are listed in the caption of Fig. 6. The  $2\sigma$  error bar applies to 1985–1998 ( $^{206}\text{Pb}/^{204}\text{Pb}$  and  $^{87}\text{Sr}/^{86}\text{Sr}$  ratios) and 1985–2005 ( $\text{SiO}_2$  contents) lavas. The  $2\sigma$  error bars for 1998–2005 Pb and Sr isotope ratios on the main plots are smaller than the size of the symbols.

changes in Pu'u 'Ō'ō lavas are inconsistent with mixing in this reservoir (Garcia *et al.*, 1996). No other suitable crustal reservoir is known to accommodate this magma mixing. Thus, crustal magma mixing is an unlikely explanation for the 1998–2003 Pu'u 'Ō'ō compositional variations. Instead, these recent lavas can be explained if they were derived from a mixture of Mauna Loa- and Kīlauea-like mantle sources that subsequently melted. This hybrid source represents a new component for the eruption.

Historical lavas from Kīlauea and Mauna Loa volcano provide an important window to the present-day composition and distribution of mantle components in the Hawaiian plume (e.g. Rhodes & Hart, 1995; Pietruszka & Garcia, 1999a). Consequently, the origin of the recent Pu'u 'Ō'ō lavas is discussed below in terms of mixing between the mantle source components defined by historical lavas from these two volcanoes (rather than the more extreme end-member isotopic compositions observed in Koʻolau and Mauna Kea lavas). The proportions of Kīlauea and Mauna Loa components in the hybrid source can be estimated from compositional mixing trends (Figs 6 and 8). The 1917 Kīlauea lava was chosen as an end member because it has the highest  $^{206}\text{Pb}/^{204}\text{Pb}$  and  $^{143}\text{Nd}/^{144}\text{Nd}$  and lowest  $^{87}\text{Sr}/^{86}\text{Sr}$  ratios among olivine-controlled historical Kīlauea lavas (Pietruszka & Garcia, 1999a). Although a range of historical Mauna Loa lavas would make reasonable isotopic end members for this calculation, the 1887 Mauna Loa lava (Rhodes & Hart, 1995) was selected because it creates a suitable mixing trend on the plots of MgO-normalized major elements vs  $^{206}\text{Pb}/^{204}\text{Pb}$  and  $^{87}\text{Sr}/^{86}\text{Sr}$  (Fig. 8). The 10-Jan-1997 Pu'u 'Ō'ō sample was chosen to represent the recently depleted Kīlauea source component because it has the lowest ratios of highly incompatible trace elements (e.g. Ba/Nb or Ba/Rb) for this eruption. Mixing trends between the 1917 Kīlauea (55%) and 1887 Mauna Loa (45%) lavas (Figs 6 and 8) pass within analytical error of the 2001–2003 Pu'u 'Ō'ō lavas (i.e. the samples with the highest  $^{87}\text{Sr}/^{86}\text{Sr}$  and MgO-normalized SiO<sub>2</sub> values). Therefore, this 55:45 Kīlauea–Mauna Loa composition might be a good estimate of the hybrid source.

This mixing model suggests that the melt contribution from the recently depleted source component decreased starting in early 1998 as melt derived from the hybrid source was tapped in greater proportions until mid-2003 (Figs 7 and 8). Following the mid-2003 compositional reversal, the lavas display chemical and isotopic variations that overlap with the compositional fields of the 1998–2003 lavas (Figs 3–8), indicating a diminishing importance for the hybrid component since 2003.

### A pyroxenite source for Pu'u 'Ō'ō lavas?

Partial melting of a heterogeneous plume source containing a mixture of peridotite and ancient recycled oceanic crust ± sediment (pyroxenite or eclogite) has become

a common explanation for the chemical and isotopic variations in Hawaiian lavas (e.g. Hauri, 1996; Lassiter & Hauri, 1998; Blichert-Toft *et al.*, 1999; Takahashi & Nakajima, 2002; Gaffney *et al.*, 2005; Sobolev *et al.*, 2005, 2007; Herzberg, 2006). For example, Koʻolau lavas, with relatively high  $^{87}\text{Sr}/^{86}\text{Sr}$  ( $\sim 0.7044$ ) and SiO<sub>2</sub> ( $\sim 53\text{--}55$  wt %), are explained by melting ancient recycled oceanic crust within the Hawaiian plume (Hauri, 1996; Lassiter & Hauri, 1998; Blichert-Toft *et al.*, 1999; Huang & Frey, 2005; Fekiacova *et al.*, 2007). Further support for a pyroxenite source within the Hawaiian plume comes from modeling compositional variations of lavas during long-lived eruptions, including Pu'u 'Ō'ō (Reiners, 2002). This model predicts that the continuous SiO<sub>2</sub> increases and CaO decreases could be explained if Pu'u 'Ō'ō lavas originated from a mixed pyroxenite–peridotite source with different solidi.

The temporal increases in  $^{87}\text{Sr}/^{86}\text{Sr}$  ratios and SiO<sub>2</sub> abundances (normalized to 10 wt % MgO) in the 1998–2003 lavas (Fig. 5) could be evidence for increased melting of an eclogite or pyroxenite lithology (i.e. recycled oceanic crust) in the Hawaiian plume. However, an increasing contribution of this source lithology during the eruption is unlikely for the following reasons. (1) The MgO-normalized SiO<sub>2</sub> trend is relatively flat prior to 1998, increased from 1998 to 2003, and has decreased since mid-2003. Moreover, the CaO trend has increased since mid-2003. Both trends are inconsistent with a simple mixed lithology source (e.g. Reiners, 2002). (2) The long-term decreases in CaO abundances (normalized to 10 wt % MgO; Fig. 5) from 1985 to 2003 suggest that there has been a decrease in the amount of clinopyroxene that is melted in the mantle source region, rather than the predicted increase of this mineral. (3) The Ni abundances of the lavas have progressively decreased (at a given MgO) from  $\sim 1992$  to 2005 (Fig. 3). Because Ni is highly compatible in olivine relative to clinopyroxene (e.g. Sobolev *et al.*, 2005), the decreases in Ni content suggest that recent Pu'u 'Ō'ō lavas originated from a peridotite source that became more olivine-rich and/or clinopyroxene-poor with time. A peridotite source is also supported by the positive correlation between  $^{226}\text{Ra}$ – $^{230}\text{Th}$  and  $^{230}\text{Th}$ – $^{238}\text{U}$  disequilibria of 1985–2001 Pu'u 'Ō'ō lavas (Pietruszka *et al.*, 2006).

### SMALL-SCALE MANTLE HETEROGENEITY

The timing of the temporal inflections of the  $^{87}\text{Sr}/^{86}\text{Sr}$  ratios in the Pu'u 'Ō'ō lavas may be used to help constrain the scale of heterogeneity within Kīlauea's melting region. The steady increase in the  $^{87}\text{Sr}/^{86}\text{Sr}$  ratios between 1998 (day  $\sim 5500$ ) and 2003 (day  $\sim 7400$ ) suggests that the proportion of the hybrid component progressively increased during this period. The lack of significant changes in the volume of magma stored in the shallow summit reservoir beneath Kīlauea during prolonged (months to years) historical

Kīlauea rift eruptions (i.e. Mauna Ulu and Pu'u 'Ō'ō) suggests that the magma supply rate is similar to lava effusion rate (Tilling *et al.*, 1987; Dvorak & Dzurisin, 1993; Denlinger, 1997). Assuming that the magma supply rate is approximately equal to the lava effusion rate ( $\sim 0.13 \text{ km}^3/\text{year}$ ; Sutton *et al.*, 2003) for the Pu'u 'Ō'ō eruption, the total volume of melt extracted from Kīlauea's source region from 1998 to 2003 ( $\sim 1900$  days) was  $\sim 0.7 \text{ km}^3$ . This estimate probably represents the maximum volume of melt derived from the hybrid source during this period. If 100% of the recently depleted and hybrid components were being tapped at the temporal inflections in 1998 and 2003, respectively, melt from the hybrid source might represent  $\sim 50\%$  of the total lava volume erupted from 1998 to 2003 ( $\sim 0.35 \text{ km}^3$ ). Models for tholeiitic basalt production within the Hawaiian plume suggest that the melt-zone porosity within Kīlauea's source region is  $\sim 2\text{--}3\%$  (Sims *et al.*, 1999; Pietruszka *et al.*, 2001). Thus, if melt tapped from 1998 to 2003 represents  $\sim 2\text{--}3\%$  of the total volume from which it was extracted, then the volume of the source region that supplied melt during this period would be  $\sim 10\text{--}35 \text{ km}^3$ .

The 1998–2003 lavas plot within analytical error along the mixing line from the recently depleted source (10-Jan-1997) towards the hybrid component (Figs 6 and 8). If these recent lavas are derived from a hybrid mantle source containing a mixture of Kīlauea and Mauna Loa components, then the size of these components must be significantly smaller than the volume of the source region that was tapped from 1998 to 2003 ( $<10\text{--}35 \text{ km}^3$ ). Thus, the Kīlauea and Mauna Loa mantle components that make up the hybrid component are thought to be mixed on a fine scale in the Hawaiian plume.

## CHEMICAL STRUCTURE OF THE HAWAIIAN PLUME

The long-term geographical and compositional differences between Hawaiian shield volcanoes have been related to the distribution of large-scale heterogeneities in a radially (Lassiter *et al.*, 1996; Bryce *et al.*, 2005), asymmetric (Abouchami *et al.*, 2005) or irregularly zoned (Kurz *et al.*, 2004) Hawaiian plume. For example, Kīlauea and Mauna Loa volcanoes have erupted geochemically distinct lavas for most of their known eruptive history, suggesting that the source components of these volcanoes (i.e. Kea and Loa) have remained compositionally distinct [except for some young prehistoric (AD 900–1400) Kīlauea and Mauna Loa lavas; Marske *et al.*, 2007] over a time scale of thousands of years (e.g. large-scale heterogeneity; Frey & Rhodes, 1993; Abouchami *et al.*, 2005). However, the recent Pu'u 'Ō'ō compositional trends suggest that both Kīlauea- and Mauna Loa-like components are present within Kīlauea's source region with a spatial distribution capable of creating the rapid fluctuation towards the hybrid composition on a time scale of years.

To explain the recent trend of Pu'u 'Ō'ō lavas towards the hybrid composition we propose a model with large-scale compositional heterogeneity (e.g. Lassiter *et al.*, 1996; DePaolo *et al.*, 2001; Bryce *et al.*, 2005) that is gradational across the Hawaiian plume (black to white shading in Fig. 9a). On a finer scale, Kīlauea- and Mauna Loa-like heterogeneities ( $<10\text{--}35 \text{ km}^3$ ) are assumed to be present (within the enlarged circles in Fig. 9a), but vary in relative abundance depending on location within the Hawaiian plume. For example, the darker zonation within Kīlauea's typical source region contains more Kīlauea heterogeneities, and vice versa for the whiter zone below Mauna Loa. Similarly, the intermediate gray zone located between these two volcanoes represents a source with approximately equal amounts of Kīlauea- and Mauna Loa-like compositions (Fig. 9a).

Resolving the spatial distribution of these small-scale compositional heterogeneities ( $<10\text{--}35 \text{ km}^3$ ) is problematic given the wide range in estimates for the size of Kīlauea's melting region. These estimates vary from an  $\sim 55 \text{ km}$  thick region near the central axis of the plume (Watson & McKenzie, 1991) to a thickness of  $<5\text{--}10 \text{ km}$  (Marske *et al.*, 2007). The maximum radius of this melting region is probably  $\sim 17 \text{ km}$  (i.e. half the distance between the summits of Kīlauea and Mauna Loa; Pietruszka *et al.*, 2001). Estimates for the rates of mantle melting in the Hawaiian plume range from  $>0.0005$  to  $>0.03 \text{ kg/m}^3$  per year (Cohen *et al.*, 1993; Hemond *et al.*, 1994; Sims *et al.*, 1999; Pietruszka *et al.*, 2001). Even the highest melting rates would require melting over a voluminous mantle source region ( $\sim 8500 \text{ km}^3$ ; Pietruszka *et al.*, 2006) to account for the vigorous lava effusion rate during the Pu'u 'Ō'ō eruption ( $\sim 0.13 \text{ km}^3/\text{year}$ ; Sutton *et al.*, 2003). Tapping such a large melting region would probably homogenize the melts derived from the three distinct sources for this eruption. Instead, the compositional variability of Pu'u 'Ō'ō lavas could be preserved if compositionally distinct melts are extracted into chemically isolated channels and efficiently transported to the surface (Pietruszka *et al.*, 2006).

The melting region beneath Hawaiian volcanoes is predicted to be zoned, with higher degrees of partial melting (and higher melt productivity) in a relatively thin zone near the top of the melting region (Watson & McKenzie, 1991). Thus, melt extraction would probably be more effective if it occurred laterally over a thinner (i.e.  $\sim 5\text{--}10 \text{ km}$  thick; Marske *et al.*, 2007) region. As melt migrates into channels to supply the Pu'u 'Ō'ō eruption, it must be extracted from more distal areas to sustain the flow of melt to the surface, otherwise the melt supply would become exhausted (Pietruszka *et al.*, 2006). In this context, we propose that the systematic geochemical trends toward the hybrid composition from 1998 to 2003 could be explained if melt pathways migrated from an area within Kīlauea's typical melting region dominated

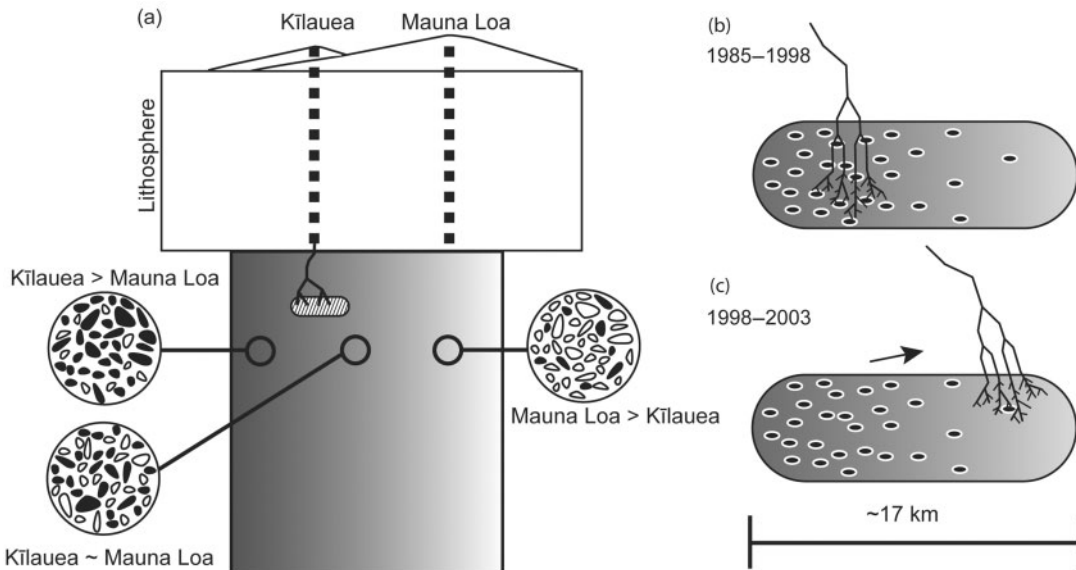


**Fig. 9.** Hypothetical cross-section of the lithosphere and the upper part of the Hawaiian plume beneath Kīlauea and Mauna Loa. (a) The long-term compositional differences between Hawaiian shield volcanoes are illustrated with black to white gradation representing large-scale compositional heterogeneity within the plume (e.g. Lassiter *et al.*, 1996; Kurz *et al.*, 2004; Abouchami *et al.*, 2005; Bryce *et al.*, 2005). Superimposed on this large-scale heterogeneity are small-scale heterogeneities ( $<10\text{--}35\text{ km}^3$ ; blobs within the enlarged circles) that reflect a predominance of Kīlauea (black) and Mauna Loa (white) components beneath these volcanoes. An isotopically distinct plume matrix (white area between the blobs) is also thought to be present in the plume based on the Pb, Sr, and Nd isotopic evidence for at least three components within the Hawaiian plume (e.g. West & Leeman, 1987; Eiler *et al.*, 1996; Hauri, 1996). The matrix is a schematic representation and other geometries of the three mantle components are possible (e.g. three isotopically distinct blobs or streaks with no matrix). Melt extraction via chemically isolated channels (inverted tree structures) may be the primary mechanism to withdraw melt from Kīlauea's melting region [striped region in (a)] into the volcano's primary magma conduit (thick dashed black line; Pietruszka *et al.*, 2006). (b) and (c) are enlargements of Kīlauea's melting region. The small-scale heterogeneities from (a) are not shown in (b) and (c) for simplicity, yet are assumed to be present. Between 1985 and 1998 (b), the recently depleted source (black ovals) was an important component in Kīlauea's melting region. The importance of the Kīlauea–Mauna Loa hybrid component (gray zone) that was progressively tapped from 1998 to 2003 can be explained if the melt channels migrated towards Mauna Loa while possibly extracting melt at shallower depths (c).

by the early and recently depleted component (black ovals; Fig. 9b) towards Mauna Loa, where more Mauna Loa-like components would be expected (Fig. 9c). In contrast, the MgO-normalized SiO<sub>2</sub> abundances are thought to be controlled by the depth of partial melting (e.g. Hirose & Kushiro, 1993; Kushiro, 1996; Longhi, 2002). Thus, the temporal increase in normalized SiO<sub>2</sub> abundances in 1998–2003 lavas could also be explained if melt production and segregation occurred at progressively shallower depths (e.g. Stolper *et al.*, 2004) during this interval (Fig. 9b and c). This model for a fine-scale mixture of compositionally distinct mantle heterogeneities (i.e. Kīlauea and Mauna Loa components) within the Hawaiian plume is consistent with the presence of both Kea and Loa compositions in young prehistoric (AD 900–1400) Kīlauea and Mauna Loa lavas (Marske *et al.*, 2007), and in the melt inclusions of East Maui lavas (Ren *et al.*, 2006).

## CONCLUSIONS

The Pu'u 'Ō'ō eruption is exceptional among historical eruptions for its long duration (25+ years) and compositional variability. The systematic geochemical fluctuations in Pu'u 'Ō'ō lavas document the short-term crustal

(e.g. crystal fractionation) and mantle (melting and source heterogeneity) processes in the Hawaiian plume. Pu'u 'Ō'ō lavas erupted from 1985 to 1998 are thought to have originated from at least two distinct source components with similar isotopic compositions, although one was more depleted in incompatible trace elements by a recent ( $<8\text{ ka}$ ) melting event in the Hawaiian plume. Post-1998 Pu'u 'Ō'ō lavas record small but distinctive variations of MgO-normalized major element abundances, and Sr isotope and incompatible trace element ratios (compared with earlier erupted lavas) that require a third source component. Lavas erupted between 1998 and 2003 display a temporal geochemical evolution toward an intermediate area between the compositional fields of historical Kīlauea and Mauna Loa lavas. Based on mixing models, the 1998–2003 Pu'u 'Ō'ō lavas trend towards a hybrid mantle source composition made of roughly equal proportions of Kīlauea- and Mauna Loa-like components. The contribution from a recently depleted Kīlauea component decreased starting in early 1998 as the volcano tapped greater proportions of a hybrid component until mid-2003. The systematic geochemical trends toward this hybrid composition can be explained if melt pathways migrated from an area within

Kīlauea's melting region (important for 1985–1998 lavas) towards Mauna Loa, where an equal mixture of Kīlauea- and Mauna Loa-like components may exist. The presence of Kīlauea (i.e. Kea) and Mauna Loa (i.e. Loa) components (<10–35 km<sup>3</sup>) in Pu'u 'Ō'ō lavas suggests that both of these components are present as a fine-scale mixture in Kīlauea's source region.

## ACKNOWLEDGEMENTS

We thank the numerous workers who collected samples for this study (especially Virginia Aragon, Kate Bridges, Eric Haskins, Bruce Houghton, Laslo Keszthely, and Scott Rowland), Chad Shishado and Nicole Robinson for assistance with the rock preparation, Michael Vollinger for the XRF preparation work and analyses, and Joan Willis for her support in the isotope clean lab at SDSU. We thank Amy Gaffney, Karen Harpp, and Mark Kurz for their helpful reviews. This research was supported by two grants from the National Science Foundation to M.O.G. and A.J.P. (EAR 03-36874 and 07-38817). This paper is SOEST Contribution 7159.

## REFERENCES

- Abouchami, W., Hofmann, A. W., Galer, S. J. G., Frey, F. A., Eisele, J. & Feigenson, M. (2005). Lead isotopes reveal bilateral asymmetry and vertical continuity in the Hawaiian mantle plume. *Nature* **434**, 851–856.
- Blichert-Toft, J., Albarède, F. & Frey, F. (1999). Hf isotopic evidence for pelagic sediments in the source of Hawaiian basalts. *Science* **285**, 879–882.
- Blichert-Toft, J., Weis, D., Maerschalk, C. & Albarède, F. (2003). Hawaiian hotspot dynamics as inferred from the Hf and Pb isotopic evolution of Mauna Kea volcano. *Geochemistry, Geophysics, Geosystems* **4**, doi:10.1029/2002GC000340.
- Bolge, L. L., Carr, M. J., Feigenson, M. D. & Alvarado, G. E. (2006). Geochemical stratigraphy and magmatic evolution at Arenal volcano, Costa Rica. *Journal of Volcanology and Geothermal Research* **157**, 34–48.
- Bryce, J. G., DePaolo, D. J. & Lassiter, J. C. (2005). Geochemical structure of the Hawaiian plume: Sr, Nd, and Os isotopes in the 2.8 km HSDP-2 section of Mauna Kea volcano. *Geochemistry, Geophysics, Geosystems* **6**, doi:10.1029/2004GC000809.
- Byers, C. D., Garcia, M. O. & Muenow, D. W. (1985). Volatiles in pillow rim glasses from Loihi and Kīlauea volcanoes, Hawaii. *Geochimica et Cosmochimica Acta* **49**, 1887–1896.
- Chen, C.-Y. & Frey, F. A. (1985). Trace element and isotopic geochemistry of lavas from Haleakala volcano, East Maui, Hawaii: implications for the origin of Hawaiian basalts. *Journal of Geophysical Research* **90**, 8743–8768.
- Chen, C.-Y., Frey, F. A., Rhodes, J. M. & Eaton, R. M. (1996). Temporal geochemical evolution of Kīlauea volcano: comparison of Hilina and Puna Basalt. In: Basu, A. & Hart, S. (eds) *Earth Processes: Reading the isotopic code*, American Geophysical Union Geophysical Monograph **95**, 161–181.
- Cohen, A. S. & O'Nions, R. K. (1993). Melting rates beneath Hawaii: evidence from uranium series isotopes in recent lavas. *Earth and Planetary Science Letters* **120**, 169–175.
- Denlinger, R. P. (1997). A dynamic balance between magma supply and eruption rate at Kīlauea volcano, Hawaii. *Journal of Geophysical Research* **102**, 18091–18100.
- DePaolo, D. J., Bryce, J. G., Dodson, A., Shuster, D. L. & Kennedy, B. M. (2001). Isotopic evolution of Mauna Loa and the chemical structure of the Hawaiian plume. *Geochemistry, Geophysics, Geosystems* **3**, doi:10.1029/2000GC000139.
- Dvorak, J. J. & Dzurisin, D. (1993). Variations in magma supply rate at Kīlauea volcano, Hawaii. *Journal of Geophysical Research* **98**, 22255–22268.
- Eaton, J. P. & Murata, K. J. (1960). How volcanoes grow [Hawaii]. *Science* **132**, 925–938.
- Eiler, J. M., Farley, K. A., Valley, J. W., Hofmann, A. W. & Stolper, E. M. (1996). Oxygen isotope constraints on the sources of Hawaiian volcanism. *Earth and Planetary Science Letters* **144**, 453–468.
- Eisele, J., Abouchami, W., Galer, S. J. G. & Hofmann, A. W. (2003). The 320 kyr Pb isotope evolution of Mauna Kea lavas recorded in the HSDP-2 drill core. *Geochemistry, Geophysics, Geosystems* **4**, doi:10.1029/2002GC000339.
- Farnetani, C. G., Legras, B. & Tackley, P. J. (2002). Mixing and deformation in mantle plumes. *Earth and Planetary Science Letters* **196**, 1–15.
- Fekiacova, A., Abouchami, W., Galer, S. J. G., Garcia, M. O. & Hofmann, A. W. (2007). Origin and temporal evolution of Koolau volcano, Hawaii: inferences from isotope data on the Koolau Scientific Drilling Project (KSDP), the Honolulu Volcanics and ODP Site 843. *Earth and Planetary Science Letters* **261**, 65–83.
- Frey, F. A. & Rhodes, J. M. (1993). Intershield geochemical differences among Hawaiian volcanoes: implications for source compositions, melting process and magma ascent paths. *Philosophical Transactions of the Royal Society of London* **342**, 121–136.
- Gaffney, A. M., Nelson, B. K. & Blichert-Toft, J. (2004). Geochemical constraints on the role of oceanic lithosphere in intra-volcano heterogeneity at West Maui, Hawaii. *Journal of Petrology* **45**, 1663–1687.
- Gaffney, A. M., Nelson, B. K. & Blichert-Toft, J. (2005). Melting in the Hawaiian plume at 1–2 Ma as recorded at Maui Nui: The role of eclogite, peridotite, and source mixing. *Geochemistry, Geophysics, Geosystems* **6**, doi:10.1029/2005GC000927.
- Galer, S. J. G. & Abouchami, W. (1998). Practical application of lead triple spiking for correction of instrumental mass discrimination. *Mineralogical Magazine* **62A**, 491–492.
- Garcia, M. O. (2002). Submarine picritic basalts from Koolau volcano, Hawaii: implications for parental magma composition and mantle source. In: Takahashi, E., Lipman, P. W., Garcia, M. O., Naka, J. & Aramaki, S. (eds) *Hawaiian Volcanoes: Deep Underwater Perspectives*. *Geophysical Monographs*, American Geophysical Union **128**, 391–401.
- Garcia, M. O., Ho, R. A., Rhodes, J. M. & Wolfe, E. W. (1989). Petrologic constraints on rift zone processes: results from episode 1 of the Puu Oo eruption of Kīlauea volcano, Hawaii. *Bulletin of Volcanology* **52**, 81–96.
- Garcia, M. O., Rhodes, J. M., Ho, R. A., Ulrich, G. & Wolfe, E. W. (1992). Petrology of lavas from episodes 2–47 of the Puu Oo eruption of Kīlauea volcano, Hawaii: evaluation of magmatic processes. *Bulletin of Volcanology* **55**, 1–16.
- Garcia, M. O., Rhodes, J. M., Trusdell, F. A. & Pietruszka, A. P. (1996). Petrology of lavas from the Puu Oo eruption of Kīlauea volcano: III. The Kupaianaha episode (1986–1992). *Bulletin of Volcanology* **58**, 359–379.
- Garcia, M. O., Ito, E., Eiler, J. & Pietruszka, A. (1998). Crystal contamination of Kīlauea volcano magmas revealed by oxygen isotope analysis of glass and olivine from the Puu Oo eruption lavas. *Journal of Petrology* **39**, 803–817.
- Garcia, M. O., Pietruszka, A. J., Rhodes, J. M. & Swanson, K. (2000). Magmatic processes during the prolonged Puu Oo eruption of Kīlauea volcano, Hawaii. *Journal of Petrology* **41**, 967–990.

- Garcia, M. O., Pietruszka, A. J. & Rhodes, J. M. (2003). A petrologic perspective of Kilauea volcano's summit magma reservoir. *Journal of Petrology* **44**, 2313–2339.
- Garcia, M. O., Ito, E. & Eiler, J. M. (2008). Oxygen isotope evidence for chemical interaction of Kilauea historical magmas with basement rocks. *Journal of Petrology* **49**, 757–769.
- Harris, A. J. L., Keszthelyi, L., Flynn, L. P., Mougins-Mark, P. J., Thornber, C., Kauahikaua, J., Sherrod, D., Trusdell, F., Sawyer, M. W. & Flament, P. (1997). Chronology of the episode 54 eruption at Kilauea volcano, Hawaii, from GOES-9 satellite data. *Geophysical Research Letters* **24**, 3281–3284.
- Hauri, E. H. (1996). Major-element variability in the Hawaiian mantle plume. *Nature* **382**, 415–419.
- Heliker, C. & Mattox, T. N. (2003). The first two decades of the Puu Oo-Kupaianaha eruption: chronology and selected bibliography. In: Heliker, C., Swanson, D. A. & Takahashi, T. J. (eds). *The Puu Oo-Kupaianaha Eruption of Kilauea Volcano, Hawaii: The First 20 Years*. US Geological Survey Professional Papers **1676**, 121–136.
- Heliker, C., Mangan, M. T., Mattox, T. N., Kauahikaua, J. P. & Helz, R. T. (1998). The character of long-term eruptions: inferences from episodes 50–53 of the Puu Oo-Kupaianaha eruption of Kilauea volcano. *Bulletin of Volcanology* **59**, 381–393.
- Hemond, C., Hofmann, A. W., Heusser, G., Condomines, M., Raczk, I. & Rhodes, J. M. (1994). U–Th–Ra systematics in Kilauea and Mauna Loa tholeiites. *Chemical Geology* **116**, 163–180.
- Herzberg, C. (2006). Petrology and thermal structure of the Hawaiian plume: a view from Mauna Kea. *Nature* **444**, 605–609.
- Hirose, K. & Kushiro, I. (1993). Partial melting of dry peridotites at high pressure: determination of composition of melts segregated from peridotite using aggregates of diamonds. *Earth and Planetary Science Letters* **114**, 477–489.
- Huang, S. & Frey, F. A. (2005). Recycled oceanic crust in the Hawaiian plume: evidence from temporal geochemical variations within the Koolau Shield. *Contributions to Mineralogy and Petrology* **149**, 556–575.
- King, A. J., Waggoner, D. G. & Garcia, M. O. (1993). Geochemistry and petrology of basalts from Leg 136, central Pacific Ocean. In: Wilkens, R. H., Firth, J., Bender, J. et al. (eds) *Proceedings of the Ocean Drilling Program, Scientific Results, 136*. College Station, TX: Ocean Drilling Program, pp. 107–118.
- Kurz, M. D. & Kammer, D. P. (1991). Isotopic evolution of Mauna Loa volcano. *Earth and Planetary Science Letters* **103**, 257–269.
- Kurz, M. D., Kenna, T. C., Kammer, D. P., Rhodes, J. M. & Garcia, M. O. (1995). Isotopic evolution of Mauna Loa Volcano: a view from the submarine southwest rift zone. In: Rhodes, J. M. & Lockwood, J. P. (eds) *Mauna Loa Revealed: Structure, Composition, History and Hazards*. American Geophysical Union Geophysical Monograph **92**, 289–306.
- Kurz, M. D., Curtice, J., Lott, D. E., III & Solow, A. (2004). Rapid helium isotopic variability in Mauna Kea shield lavas from the Hawaiian Scientific Drilling Project. *Geochemistry, Geophysics, Geosystems* **5**, doi:10.1029/2002GC000439.
- Kushiro, I. (1996). Partial melting of fertile mantle peridotite at high pressures: an experimental study using aggregates of diamond. In: Basu, A. & Hart, S. (eds) *Earth Processes: Reading the isotopic code*. American Geophysical Union Geophysical Monograph **95**, 109–122.
- Lassiter, J. C. & Hauri, E. H. (1998). Osmium-isotope variations in Hawaiian lavas: evidence for recycled oceanic lithosphere in the Hawaiian plume. *Earth and Planetary Science Letters* **164**, 483–496.
- Lassiter, J. C., DePaolo, D. J. & Tatsumoto, M. (1996). Isotopic evolution of Mauna Kea volcano: results from the initial phase of the Hawaii Scientific Drilling Project. *Journal of Geophysical Research* **101**, 11769–11780.
- Longhi, J. (2002). Some phase equilibria systematics of lherzolite melting: I. *Geochemistry, Geophysics, Geosystems* **2**, doi:10.1029/2001GC000204.
- Macdonald, G. A., Abbott, A. T. & Peterson, F. L. (1983). *Volcanoes in the Sea: the Geology of Hawaii*. Honolulu, HI: University of Hawaii Press.
- Marske, J. P., Pietruszka, A. J., Weis, D., Garcia, M. O. & Rhodes, J. M. (2007). Rapid passage of a small-scale heterogeneity through the melting regions of Kilauea and Mauna Loa volcanoes, Hawaii. *Earth and Planetary Science Letters* **259**, 34–50.
- McBirney, A. R., Taylor, H. P. & Armstrong, R. L. (1987). Paricutin re-examined; a classic example of crustal assimilation in calc-alkaline magma. *Contributions to Mineralogy and Petrology* **95**, 4–20.
- McKenzie, D. (1985).  $^{230}\text{Th}$ – $^{238}\text{U}$  disequilibrium and the melting processes beneath ridge axes. *Earth and Planetary Science Letters* **72**, 149–157.
- Mittelstaedt, E. & Garcia, M. O. (2007). Modeling the sharp compositional interface in the Puu Oo magma reservoir, Kilauea volcano, Hawaii. *Geochemistry, Geophysics, Geosystems* **8**, doi:10.1029/2006GC001519.
- Moore, J. G. & Ault, W. U. (1965). Historic littoral cones in Hawaii. *Pacific Science* **19**, 3–11.
- Nakata, J. S., Heliker, C. & Sherrod, D. R. (2000). Hawaiian Volcano Observatory; Summary 99; Part 1, Seismic data, January to December 1999, with a chronological summary. US Geological Survey Report **OF 00-0433**, 61 pp.
- Norman, M. D., Griffin, W. L., Pearson, N. J., Garcia, M. O. & O'Reilly, S. Y. (1998). Quantitative analysis of trace element abundances in glasses and minerals: a comparison of laser ablation ICPMS, solution ICPMS, proton microprobe, and electron microprobe data. *Journal of Analytical Atomic Spectrometry* **13**, 477–482.
- Okano, O. & Tatsumoto, M. (1996). Petrogenesis of ultramafic xenoliths from Hawaii inferred from Sr, Nd, and Pb isotopes. In: Basu, A. & Hart, S. (eds) *Earth Processes: Reading the isotopic code*. American Geophysical Union Geophysical Monograph **95**, 135–147.
- Pietruszka, A. P. & Garcia, M. O. (1999a). A rapid fluctuation in the mantle source and melting history of Kilauea volcano inferred from the geochemistry of its historical summit lavas (1790–1982). *Journal of Petrology* **40**, 1321–1342.
- Pietruszka, A. P. & Garcia, M. O. (1999b). The size and shape of Kilauea volcano's summit magma storage reservoir: a geochemical probe. *Earth and Planetary Science Letters* **167**, 311–320.
- Pietruszka, A. P., Rubin, K. H. & Garcia, M. O. (2001).  $^{226}\text{Ra}$ – $^{230}\text{Th}$ – $^{238}\text{U}$  disequilibria of historical Kilauea lavas (1790–1982) and the dynamics of mantle melting within the Hawaiian plume. *Earth and Planetary Science Letters* **186**, 15–31.
- Pietruszka, A. J., Hauri, E. H., Carlson, R. W. & Garcia, M. O. (2006). Remelting of recently depleted mantle within the Hawaiian plume inferred from the  $^{226}\text{Ra}$ – $^{230}\text{Th}$ – $^{238}\text{U}$  disequilibria of Puu Oo eruption lavas. *Earth and Planetary Science Letters* **244**, 155–169.
- Poland, M., Miklius, A., Orr, T., Sutton, J., Thornber, D. & Wilson, D. (2008). New episodes of volcanism at Kilauea volcano, Hawaii. *EOS Transactions, American Geophysical Union* **89**, 37–38.
- Powers, H. (1955). Composition and origin of basaltic magma of the Hawaiian Islands. *Geochimica et Cosmochimica Acta* **7**, 77–107.
- Putirka, K. (1997). Magma transport at Hawaii: inferences based on igneous thermobarometry. *Geology* **25**, 69–72.
- Reiners, P.W. (2002). Temporal–compositional trends in intraplate basalt eruptions: implications for mantle heterogeneity and melting processes. *Geochemistry, Geophysics, Geosystems* **3**, doi:10.1029/2001GC000250.
- Ren, Z.-Y., Tomoyuki, S., Masako, Y., Johnson, K. M. & Takahashi, E. (2006). Isotope compositions of submarine Hana Ridge lavas, Haleakala volcano, Hawaii: Implications for source compositions,

- melting process and the structure of the Hawaiian plume. *Journal of Petrology* **47**, 255–275.
- Rhodes, J. M. (1996). Geochemical stratigraphy of lava flows sampled by the Hawaii Scientific Drilling Project. *Journal of Geophysical Research* **101**, 11729–11746.
- Rhodes, J. M. & Hart, S. R. (1995). Episodic trace element and isotopic variations in historical Mauna Loa lavas: implications for magma and plume dynamics. In: Rhodes, J. M. & Lockwood, J. P. (eds) *Mauna Loa Revealed: Structure, Composition, History and Hazards*. American Geophysical Union Geophysical Monograph **92**, 263–288.
- Rhodes, J. M. & Vollinger, M. J. (2004). Composition of basaltic lavas sampled by phase-2 of the Hawaii Scientific Drilling Project: Geochemical stratigraphy and magma types. *Geochemistry, Geophysics, Geosystems* **5**, doi:10.1029/2002GC000434.
- Rhodes, J. M. & Vollinger, M. J. (2005). Ferric/ferrous ratios in 1984 Mauna Loa lavas: a contribution to understanding the oxidation state of Hawaiian magmas. *Contributions to Mineralogy and Petrology* **149**, 666–674.
- Rhodes, J. M., Wenz, K. P., Neal, C. A., Sparks, J. W. & Lockwood, J. P. (1989). Geochemical evidence for invasion of Kilauea's plumbing system by Mauna Loa magma. *Nature* **337**, 257–260.
- Rizzo, A., Caracausi, A., Favara, R., Martelli, M., Paonita, A., Paternoster, M., Nuccio, P. M. & Rosciglione, A. (2006). New insights into magma dynamics during the last two eruptions of Mount Etna as inferred by geochemical monitoring from 2002 to 2005. *Geochemistry, Geophysics, Geosystems* **7**, doi:10.1029/2005GC001175.
- Roeder, P. L. & Emslie, R. F. (1970). Olivine–liquid equilibrium. *Contributions to Mineralogy and Petrology* **29**, 275–289.
- Shamberger, P. J. & Garcia, M. O. (2006). Geochemical modeling of magma mixing and magma reservoir volumes during early episodes of Kilauea volcano's Puu Oo eruption. *Bulletin of Volcanology* **69**, 345–352.
- Sigmarsson, O., Karlsson, H. R. & Larsen, G. (2000). The 1996 and 1998 subglacial eruptions beneath the Vatnajokull ice sheet in Iceland: contrasting geochemical and geophysical inferences on magma migration. *Bulletin of Volcanology* **61**, 468–76.
- Sims, K. W. W., DePaolo, D. J., Murrell, M. T., Baldridge, W. S., Goldstein, S., Clague, D. & Jull, M. (1999). Porosity of the melting zone and variations in the solid mantle upwelling rate beneath Hawaii: inferences from the  $^{238}\text{U}$ – $^{230}\text{Th}$ – $^{226}\text{Ra}$  and  $^{235}\text{U}$ – $^{231}\text{Pa}$  disequilibrium. *Geochimica et Cosmochimica Acta* **63**, 4119–4138.
- Sobolev, A. V., Hofmann, A. W., Sobolev, S. V. & Nikogosian, I. K. (2005). An olivine-free mantle source of Hawaiian shield basalts. *Nature* **434**, 590–597.
- Sobolev, A. V., Hofmann, A. W., Kuzmin, D. V., Yaxley, G. M., Arndt, N. T., Chung, S.-L., Danyushevsky, L. V., Elliott, T., Frey, F. A., Garcia, M. O., Gurenko, A. A., Kamenetsky, V. S., Kerr, A. C., Krivolutskaya, N. A., Matvienkov, V. V., Nikogosian, I. K., Rocholl, A., Sigurdsson, I. A., Sushchevskaya, N. M. & Teklay, M. (2007). The amount of recycled crust in sources of mantle-derived melts. *Science* **316**, 412–417.
- Stille, P., Unruh, D. M. & Tatsumoto, M. (1986). Pb, Sr, Nd, and Hf isotopic constraints on the origin of Hawaiian basalts and evidence for a unique mantle source. *Geochimica et Cosmochimica Acta* **50**, 2303–2319.
- Stolper, E. M., DePaolo, D. J. & Thomas, D. M. (1996). Introduction to special section: Hawaii Scientific Drilling Project. *Journal of Geophysical Research* **101**, 11593–11598.
- Stolper, E. M., Sherman, S., Garcia, M. O., Baker, M. & Seaman, C. (2004). Glasses in the submarine section of the HSDP-2 drill core, Hilo, Hawaii. *Geochemistry, Geophysics, Geosystems* **5**, doi:10.1029/2003GC000553.
- Sutton, J. A., Elias, T. & Kauahikaua, J. (2003). Lava-effusion rates for the Puu Oo–Kupaianaha eruption derived from SO<sub>2</sub> emissions and very low frequency (VLF) measurements. In: Heliker, C., Swanson, D. A. & Takahashi, T. J. (eds) *The Puu Oo–Kupaianaha Eruption of Kilauea Volcano, Hawaii: the First 20 Years*. US Geological Survey Professional Papers **1676**, 121–136.
- Takahashi, E. & Nakajima, K. (2002). Melting process in the Hawaiian plume; an experimental study. In: Takahashi, E., Lipman, P. W., Garcia, M. O., Naka, J. & Aramaki, S. (eds) *Hawaiian Volcanoes: Deep Underwater Perspectives*. American Geophysical Union, Geophysical Monographs **128**, 403–418.
- Tatsumoto, M. (1978). Isotopic composition of lead in oceanic basalt and its implication to mantle evolution. *Earth and Planetary Science Letters* **38**, 63–87.
- Thirlwall, M. F. (2002). Multicollector ICP-MS analysis of Pb isotopes using a  $^{207}\text{Pb}$ – $^{204}\text{Pb}$  double spike demonstrates up to 400 ppm/amu systematic errors in Ti-normalization. *Chemical Geology* **184**, 255–274.
- Thornber, C. R. (2001). Olivine–liquid relations of lava erupted by Kilauea volcano from 1994 to 1998: implications for shallow magmatic processes associated with the ongoing East-Rift-Zone eruption. *Canadian Mineralogist* **39**, 239–266.
- Thornber, C. R. (2003). Magma-reservoir processes revealed by geochemistry of the Puu Oo–Kupaianaha eruption. In: Heliker, C., Swanson, D. A. & Takahashi, T. J. (eds) *The Puu Oo–Kupaianaha Eruption of Kilauea Volcano, Hawaii: the First 20 Years*. US Geological Survey Professional Papers **1676**, 121–136.
- Thornber, C. R., Heliker, C., Sherrod, D. R., Kauahikaua, J. P., Miklius, A., Okubo, P. G., Trusdell, F. A., Budahn, J. R., Ridley, W. I. & Meeker, G. P. (2003). Kilauea East Rift Zone magmatism; an episode 54 perspective. *Journal of Petrology* **44**, 1525–1559.
- Tilling, R. I. & Dvorak, J. J. (1993). Anatomy of a basaltic volcano. *Nature* **363**, 125–133.
- Tilling, R. I., Wright, T. L. & Millard, H. T. Jr (1987). Trace-element chemistry of Kilauea and Mauna Loa lava in space and time: a reconnaissance. In: Decker, R. W., Wright, T. L. & Stauffer, P. H. (eds) *Volcanism in Hawaii*. US Geological Survey Professional Paper **1350**, 641–689.
- Ulmer, P. (1989). The dependence of the Fe<sup>2+</sup>–Mg cation-partitioning between olivine and basaltic liquid on pressure, temperature and composition. *Contributions to Mineralogy and Petrology* **101**, 261–271.
- Vlastelic, I., Staudacher, T. & Semet, M. (2005). Rapid change of lava composition from 1998 to 2002 at Piton de la Fournaise (Reunion) inferred from Pb isotopes and trace elements; evidence for variable crustal contamination. *Journal of Petrology* **46**, 79–107.
- Wanless, V. D., Garcia, M. O., Trusdell, F. A., Rhodes, J. M., Norman, M. D., Weis, D., Fornari, D. J., Kurz, M. D. & Guillou, H. (2006). Submarine radial vents on Mauna Loa volcano, Hawaii. *Geochemistry, Geophysics, Geosystems* **7**, doi:10.1029/2005GC001086.
- Watson, S. & McKenzie, D. (1991). Melt generation by plumes: a study of Hawaiian volcanism. *Journal of Petrology* **32**, 501–537.
- West, H. B. & Leeman, W. P. (1987). Isotopic evolution of lavas from Haleakala volcano, Hawaii. *Earth and Planetary Science Letters* **84**, 211–225.
- Wilcox, R. E. (1954). Petrology of Paricutin volcano, Mexico. *US Geological Survey Bulletin* **B 0965-C**, 281–354.
- Williams, R. W. & Gill, J. B. (1989). Effects of partial melting on the uranium decay series. *Geochimica et Cosmochimica Acta* **53**, 1607–1619.
- Wolfe, E. W., Garcia, M. O., Jackson, D. B., Koyanagi, R. Y., Neal, C. A. & Okamura, A. T. (1987). The Puu Oo eruption of Kilauea volcano, episodes 1 through 20, January 3, 1983, to June 8,

1984. In: Decker, R. W., Wright, T. L. & Stauffer, P. H. (eds) *Volcanism in Hawaii, United States Geological Survey Professional Paper 1350*, 471–508.
- Wright, T. L. (1971). Chemistry of Kilauea and Mauna Loa in space and time. *United States Geological Survey Professional Paper 735*, 1–40.
- Wright, T. L. & Klein, F. W. (2006). Deep magma transport at Kilauea Volcano, Hawaii. *Lithos* **87**, 50–79.
- Xu, G., Frey, F. A., Clague, D. A., Abouchami, W., Blichert-Toft, J., Cousens, B. & Weisler, M. (2007). Geochemical characteristics of West Molokai shield- and postshield-stage lavas: constraints on Hawaiian plume models. *Geochemistry, Geophysics, Geosystems* **8**, doi:10.1029/2006GC001554.

## APPENDIX

*Table A1: Sr isotope ratios for Pu'u 'O'o lavas*

Sample	$^{87}\text{Sr}/^{86}\text{Sr}$ (TIMS)	$^{87}\text{Sr}/^{86}\text{Sr}$ (MC-ICP-MS)	Sample	$^{87}\text{Sr}/^{86}\text{Sr}$ (TIMS)	$^{87}\text{Sr}/^{86}\text{Sr}$ (MC-ICP-MS)	Sample	$^{87}\text{Sr}/^{86}\text{Sr}$ (TIMS)	$^{87}\text{Sr}/^{86}\text{Sr}$ (MC-ICP-MS)	Sample	$^{87}\text{Sr}/^{86}\text{Sr}$ (TIMS)	$^{87}\text{Sr}/^{86}\text{Sr}$ (MC-ICP-MS)
26-Mar-89	0.703586		27-Oct-99	0.703610	0.703627	15-Jan-04	0.703625	0.703642	Kil1919	0.703472	
	0.703582			0.703619			0.703634			0.703476	
	0.703581			0.703630			0.703638			0.703483	
12-May-91	0.703586		19-Feb-00	0.703617	0.703634		0.703623				
				0.703623							
29-Dec-92 #1	0.703606			0.703621		7-Jun-04	0.703623	0.703635			
	0.703585						0.703627				
	0.703598		21-Jun-00		0.703644		0.703621				
				8-Jan-01		0.703639		0.703612			
29-Dec-92 #2	0.703609		7-Jul-01	0.703616	0.703635	31-Jan-05	0.703622				
	0.703591			0.703631			0.703627				
	0.703594			0.703621			0.703616				
27-Apr-95	0.703594		9-Feb-02	0.703636	0.703628		0.703622				
	0.703612			0.703646			0.703616				
	0.703598			0.703639			0.703634				
7-Sep-98	0.703607		20-Aug-02	0.703642	0.703633		0.703629				
	0.703592			0.703638							
	0.703607			0.703643		8-Aug-05	0.703620				
	0.703602						0.703631				
	0.703592		12-Apr-03	0.703634	0.703641		0.703611				
	0.703608			0.703643			0.703613				
				0.703644			0.703641				
13-Feb-99		0.703616					0.703613				

Multiple analyses for a given sample are from a single dissolution. The average  $^{87}\text{Sr}/^{86}\text{Sr}$  value for each sample is presented in Table 5. Samples 26-Mar-89, 12-May-91, 29-Dec-92 (#1 and #2), and 27-Apr-95 were re-run to further improve the precision of these analyses compared with the data presented by Garcia *et al.* (1996, 2000) and Pietruszka *et al.* (2006). Samples 29-Dec-92 #1 and #2 represent separate dissolutions performed by Pietruszka *et al.* (2006). The  $^{87}\text{Sr}/^{86}\text{Sr}$  values of the SRM987 standard by TIMS were  $0.710255 \pm 17$  ( $2\sigma$ ;  $n=60$ ) for the 1999–2004 Pu'u 'O'o lavas, and  $0.710246 \pm 17$  ( $2\sigma$ ;  $n=18$ ) for Kil1919 and the 1989–1998 and 2005 Pu'u 'O'o lavas. Multiple analyses of the SRM987 standard by MC-ICP-MS with the 1998–2004 lavas gave  $^{87}\text{Sr}/^{86}\text{Sr} = 0.710220 \pm 13$  ( $2\sigma$ ;  $n=35$ ). The in-run errors are less than the external reproducibility of SRM987. All Sr isotope ratios are reported relative to  $^{87}\text{Sr}/^{86}\text{Sr} = 0.710250$  for SRM987.